Project	**IEEE 802.20 Working Group on Mobile Broadband Wireless Access** <http://ieee802.org/20/>
Title	**QTDD Performance Report 2**
Date Submitted	**2005-11-15**
Source(s)	Jim Tomcik Qualcomm, Incorporated 5775 Morehouse Drive San Diego, CA, 92121 Voice: 858-658-3231 Fax: 858-658-2113 E-Mail: jtomcik@qualcomm.com
Re:	MBWA Call for Proposals
Abstract	This contribution (part of the QTDD proposal package for 802.20), contains the QTDD Performance Report 2.
Purpose	For consideration of 802.20 in its efforts to adopt a TDD proposal for MBWA.
Notice	
Release	
Patent Policy	

QTDD Performance Report 2

This report describes the performance of the following aspects of the QTDD proposal.

- System performance under a mix of offered traffic (FTP, HTTP, Voice and NRTV)
  - Modeling of the overhead channels
  - Performance of various traffic classes
  - Link simulation results for high mobility channels not included in the channel mix for the traffic models.
- System performance under mobility
  - Handoff
  - Idle State Performance
- Performance enhancement techniques

1 Traffic Mix Evaluation

1.1 Introduction

This section reports on the performance tests of (a) System Scheduler, (b) RLP, (c) TCP/IP, and (d) Traffic models, specifically, FTP, HTTP, NRTV, and VOIP as described in [1]. Traffic model calibration is described in Report 1; please refer to [6] for the results of that testing procedure. The simulation parameters for this evaluation appear in Table 1-1.

Table 1-1 Parameters for Packet Performance Evaluation

	FL Evaluation	RL Evaluation
QoS Admission Control	30-30-30-10% Per-sector FTP-HTTP-NRTV-VoIP	VoIP
TCP Packet Size	1500 bytes	N/A
Maximum RLP Transmissions	1(VOIP), 2(Others)	1
Simulation Time	5:00 minutes	5:00 minutes

We summarize the important parameters of these traffic models in Table 1-2, see [1] and [9] for details. In this table we use HTTP as the base model and cast the other 3 models into the HTTP framework, which includes a main page transfer, main page parsing delay, several embedded page (picture) transfers, and then a reading or think-time/idle-time before a new transfer. The "average demand" in this table is calculated under an assumption that the air interface is infinitely fast. The scheduler should serve high priority traffic models at their average demand.

Table 1-2 Traffic Model Parameters

	VOIP	NRTV	FTP	HTTP	
main page size	14	-	2000000‡	‡ 10710	bytes (mean)
embedded page size	-	‡ 100	-	‡ 7758	bytes (mean)
embedded pages	-	8	-	‡ 5.64	pages (mean)
total size	112	6400	16000000	435721	bits (mean)
embedded delay	-	†‡ 0.006	-	†‡ 0.130	secs (mean)
reading/think-time delay	0.010	0.100	†‡ 180.000	†‡ 30.000	secs (mean)
total delay	0.010	0.100	180.000	30.130	secs (mean)
average demand	11200	‡ 64000	‡ 88888	‡14461	bits/s (mean)
variance	none	low	high	high	bits/s (mean)
mix weight	0.10	0.30	0.30	0.30	
weighted avg. demand	51325				bits/s (mean)

‡ - random variable (other parameters are constants)

† - this delay is adaptive, i.e. it begins when the previous transfer is completed (others are fixed periodic). NRTV releases 8 packets within 100 ms, with an inter-arrival of 6 ms, which does not affect total delay.

1.2 Channel Mixes

Traffic mix simulations with channel mix have been performed to satisfy the requirements of the Evaluation Criteria [1]. Figure 1-1 shows the average served mobile throughput for each QoS flow type and channel model combination under the assumption of 10 users per sector and 19 cells wrap-around layout. In all of these simulations, the air-interface is underloaded, typically at less than 10% utilization. The FTP throughput of this simulation exceeds that of Table 1-2 because 360 FTP transfers were completed, whereas only 283 would normally be expected in a 5 minute period.

All additional simulation results in the rest of this section will use suburban macro channel model based on the observation that system performance is roughly invariant to the channel mix.

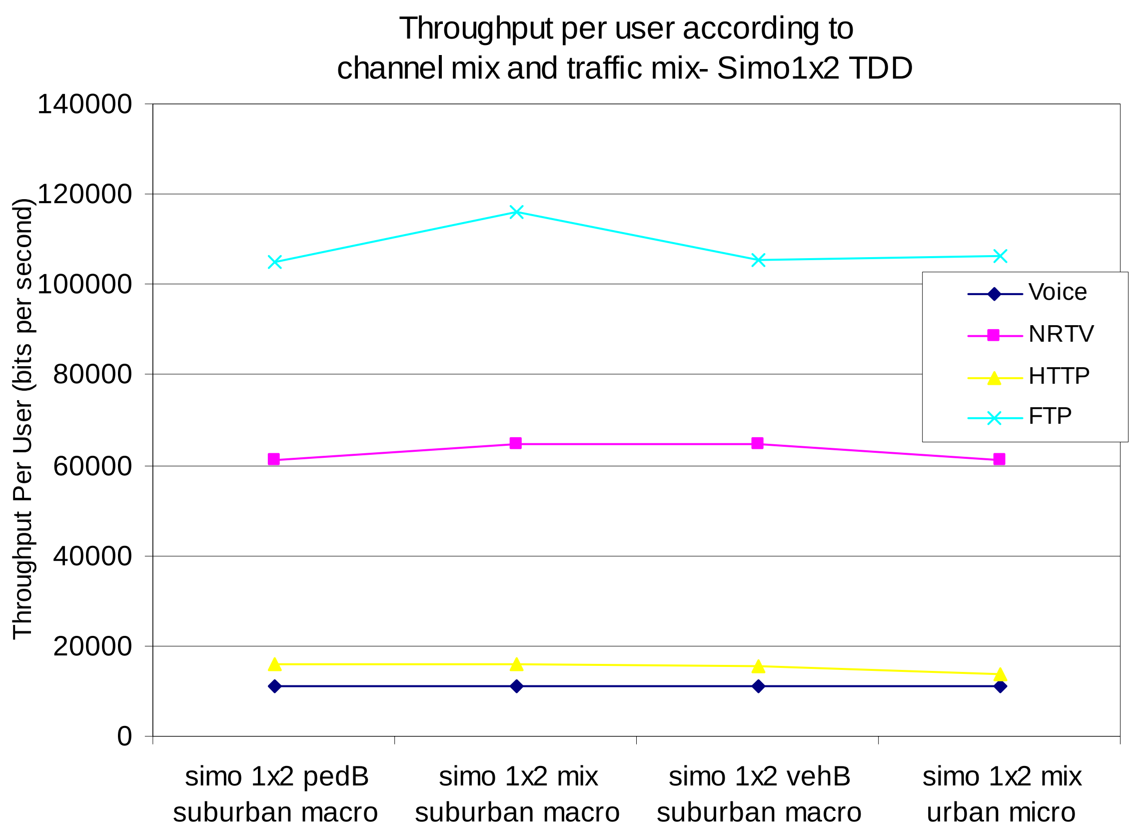

Figure 1-1 Average served mobile throughput according to traffic and channel mix with system load of 10 users per sector

1.3 Overhead Channels

This section describes the modeling of the overhead channels, and their effect on the traffic mix performance.

1.3.1 Overhead Modeling in the System Simulation

Forward link operation involves the use of the following channels.

1. F-DCH: This channel is modeled exactly
2. F-SSCH: This channel is assumed to have no errors. The effect of errors on offered traffic is described separately in 1.3.3. Interference from other sectors (due to SSCH) is modeled conservatively, as described in Section 1.2.3.1 of [6]. The assignment capacity of this channel is assumed to be finite as described in the next section.
3. R-ACKCH: This channel is assumed to have no errors. The effect of errors on offered traffic is described separately in 1.3.3.

Reverse link power control affects the FL simulation through the reverse control channels. The reverse control channels in the proposals are power controlled such that the erasure rate on the R-CQI channel is at a fixed target. When the erasure rate on the R-CQI channel is at this fixed target, the error rate on the reverse control channels are as shown in Table 1-4.

Reverse link operation involves the use of the following channels.

1. R-CQICH modeled (RL power control modeled exactly)

2. R-REQCH assumed to have no errors.

3. F-ACKCH assumed to have no errors.

1.3.2 Overhead Calculation

This section calculates the overhead due to the SSCH on the forward link.

1.3.2.1 Assignment Sizing in TDD

The system simulation assumes a capacity of 18 assignments per SSCH in a frame. In the event of the scheduler is unable to send all required assignments due to assignment capacity limitation (power or bandwidth) of the SSCH, the scheduler uses advanced features, such as sticky assignments, to cope with assignment constraints.

The performance of a scheduler with sticky assignments is illustrated in Table 1-3. It is observed that only up to 1.5% of additional traffic channel resources go unused in case the scheduler is unable to send enough assignments under the maximum 12 FLAB constraint. In the simulation results presented in the rest of the report, we limit the scheduler to send at most 12 FLABs and 6 RLABs per interlace.

Table 1-3 FL resource utilization with maximum FLAB constraint

Resource Utilization	Number of Users		
	100	160	220
No Assignment Limitation	97.3%	99.9%	100%
Maximum 12 FLABs	97.3%	98.4%	99.4%
Maximum 8 FLABs	95.7%	94.7%	96.9%
Maximum 4 FLABs	78.4%	86.3%	89.6%

1.3.2.2 Percentage Overhead in TDD

For the forward link, a 10% SSCH overhead is assumed to support 200 users. The SSCH structure is described in [7] and [5]. The SSCH has the following components

Power Control: Each power control command occupies one modulation symbol of the SSCH, and the number of power control symbols per SSCH in a frame is given by

PCSymbolsPerFrame = ceil(MACIDRange/FLPCReportInterval)

With MACIDRange = 255 and FLPCReportInterval=6 Frames (i.e. PC bits are sent to each user once in every 6 FL Frames), PCSymbolsPerFrame can be seen to be 44.

Acknowledgement: The number of base nodes in a 10 MHz system is 62, and with three modulation symbols per base node, acknowledgements require 186 modulation symbols per SSCH in a frame.

Assignment: 18 Assignment blocks at a spectral efficiency of 1 are assumed. Given that each assignment block consists of 49 bits (for 10MHz system, assuming a 8 bit ChannelID and including a 16 bit CRC), each assignment block requires 49 modulation symbols. Therefore, 18 assignment blocks require 18*49=882 symbols.

Adding the above three contributors gives 44+186+882=1112 modulation symbols. The physical layer allows for 110 modulation symbols for each 16 carriers allotted to the SSCH. Thus, the SSCH will require 11 sets of 16 carriers to accommodate 1118 modulation symbols. Since there are 64 available sets of 16 carriers, the overhead is 11/64 = 17.2%.

1.3.3 Effect of signaling errors on simulation results

1.3.3.1 Traffic with Reliable Transport and average three HARQ transmissions

The effect of signaling errors is modeled by increased delay at the application level. The contribution of various types of errors on the delay is given below. For simplicity, it is assumed that multiple error events do not occur during transmission of a packet. This is a reasonable assumption because the error events have low probability.

ACK → NACK Error (on other than last HARQ): This error causes the access network to transmit one extra HARQ attempt. The extra HARQ attempt results in extra delay for subsequent packets, and for the file in transmission, delay increase is 1 HARQ interval. The ACK channel is designed to attain NACK→ACK error rate of 0.001 and ACK→NACK error rate of 0.01.

ACK → NACK Error (on last HARQ): This error causes the access network to retransmit the entire packet. Retransmission constitutes an additional delay of three HARQ intervals. Further, there may be an assignment delay, and a conservative value of 1 HARQ interval is assumed here. Thus, the delay increase from this error is 4 HARQ intervals.

NACK → ACK Error: For applications with reliable RLP transport (such as HTTP or FTP), a NACK to ACK error causes the access terminal to send a RLP NAK message that in turn causes the access network to retransmit the packet. The extra delay in this process consists of three parts

- Access terminal determines that an error has occurred: 6 HARQ intervals
- Access terminal sends RLP NACK: 2 HARQ intervals for sending request for reverse link assignment, followed by 3 HARQ intervals for sending RLP NACK
- Access network resends the packet: 3 HARQ intervals

This constitutes a delay increase of 15 HARQ intervals

Missed FLAB: The access network becomes aware of the error after making 6 HARQ attempts, and then resends the packet. There may be an assignment delay before the access network is able to resend the packet, and a conservative value of 1 HARQ interval is assumed here. This constitutes a delay increase of 7 HARQ intervals. The probability of a FLAB being missed may be controlled by the access network because the system allows independent power allocation to different assignments, and the access network may set the power to attain the required error rate.

CQI Error: This error occurs when the access terminal's reported CQI is decoded in error at the access network, and a higher than requested packet format is used for transmission, resulting in packet error. This error results in a delay increase of 7 HARQ intervals (same argument as missed FLAB).

Table 1-4 Effect of error events on delay assuming termination in 3 attempts

Type of Error	Probability	Delay increase	
		Number of HARQ intervals	Time (ms)
ACK → NACK (not last HARQ)	0.02	1	5.47
ACK → NACK (last HARQ)	0.01	4	21.87
NACK → ACK	0.001	15	82.03
Missed FLAB	0.01[1]	7	38.28
CQI Error	0.001	7	38.28
Weighted Total per packet		**0.152**	**0.83**

From the above table, it follows that for a typical single packet that requires three HARQ attempts to transmit, the effect of errors is approximately 0.83/(5.47*2) = 7.5%. However, the effect is smaller on actual traffic models. See 1.4.1.1 for details.

[1] This is a worst case assumption, and the access network should be able to attain lower error probabilities on FLABs.

1.3.3.2 Traffic with Unreliable Transport

1.3.3.2.1 Forward Link

Traffic with unreliable transport is not retransmitted by the RLP in case of error in the first transmission attempt. In this case, the following signaling errors will result in a packet error

1. Missed FLAB error

2. CQI error

Since none of the errors above are modeled in the system simulation, the packet error rate seen at the application will be the sum of the packet error rate measured during the system simulation and the probabilities of the above errors.

For RLP unreliable transport, assignment management is done in a way that causes the probability of missed FLAB to be less than 0.001. This is done by targeting assignment blocks corresponding to users with unreliable transport with a power such that an error rate of 0.001 is attained.

The CQI error probability is 0.001 according to the CQI power control design (see 3.2.1 in [7]). This brings the total error probability contributed by signaling to 0.002.

Traffic with unreliable transport does not suffer from extra delay caused by signaling errors.

1.3.3.2.2 Reverse Link

A Missed RLAB signaling error results in a packet error. Similar to the FLAB, the probability of RLAB signaling error is 0.001.

Traffic with unreliable transport does not suffer from extra delay caused by signaling errors.

1.4 Scheduler Fairness

The system scheduler arbitrates among flows with QoS reservations (VOIP, NRTV), and flows without reservations (HTTP, FTP). The scheduler implements the IP service classes EF (expedited forwarding), AF (assured forwarding), and BE (best effort), and assigns VOIP to the EF class; NRTV to the AF class; and HTTP/FTP to the BE class. This gives VOIP flows strictly higher priority than NRTV flows, and gives NRTV flows strictly higher priority than HTTP or FTP flows. In addition, EF flow packets are not retransmitted, whereas AF and BE packets are retransmitted.

1.4.1 Mean Transfer Latency According to Load

When the admission control system accepts a QoS reservation, the scheduler is responsible for transmitting flow packets before the requested packet deadline.

VOIP. The ITU recommends a budget of 150 milliseconds for mouth-ear voice communications. This budget is further subdivided into local backhaul (50 ms), national backhaul (50 ms), and remote local backhaul (50 ms). For our evaluation, we assume that the voice deadline is 100 ms minus the associated local overheads (10 ms for backhaul, 10 ms for sampling, 5 ms for speech coding and MAC/PHY coding.) Thus, it is important for the air interface to deliver voice traffic in 75 ms or less.

NRTV. The proposed NRTV application includes a 5 second de-jitter and playback buffer. If the buffer runs dry then the video freezes and the NRTV player is in outage.

HTTP. HTTP is not a hard real-time QoS application but latency plays a key role in successful HTTP transmission. However, the HTTP model has a mean main-page size of 10,700 bytes and a variance of 25,034 bytes so the size of the main page is highly variable.

FTP. Mobile perceived download speed is the main application requirement for FTP. The FTP traffic model transfer size often varies from 1.5 Mb to 3.5Mb. Therefore, the latencies for FTP that we report are not indicative of user experience; refer to Figure 1-4 for user experience for FTP.

The latency performance of our system scheduler is depicted in Figure 1-2. As shown in the figure, Voice users experience less than 10ms air-interface latency, which is negligible compared to the 100ms QoS requirement, for all tested system load of up to 200 users. NRTV users experience mean latency much lower than the 5 seconds outage criteria for all tested system load of up to 200 users. Note that while the mean latency of voice user remains almost constant, the NRTV latency increases with the system load. HTTP users are shown to have good quality of service when system is moderately loaded, but user experience degrades significantly at higher load. Different QoS reservation and scheduling schemes could be implemented to limit the total capacity taken by EF and AF traffic so that BE traffic is not completely starved.

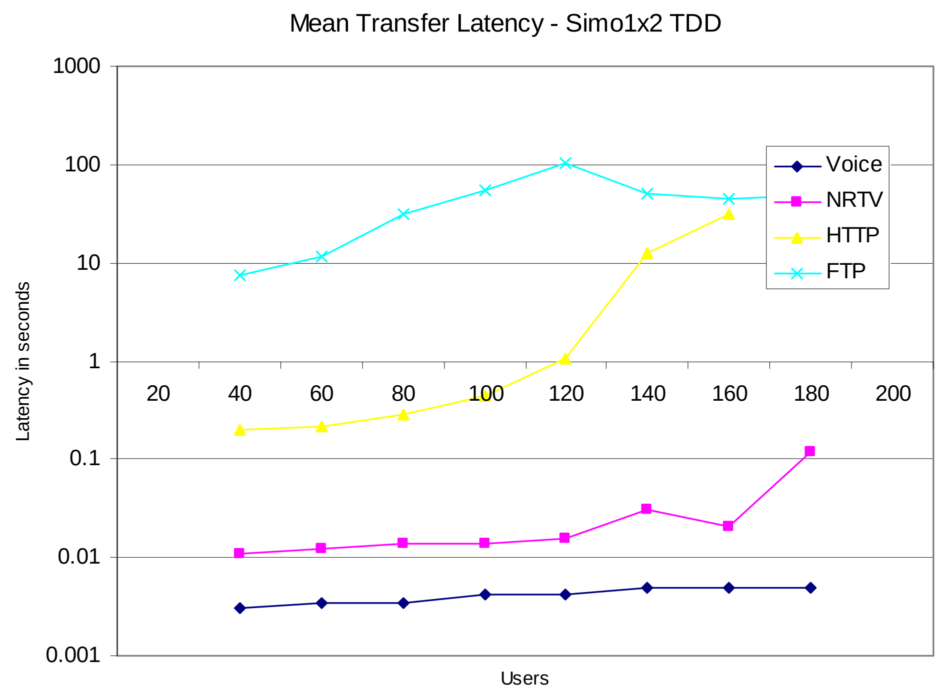

Figure 1-2 Mean transfer latency according to load, 30-30-30-10% loading

1.4.1.1 Effect of signaling errors for application models

The effect of signaling errors for single packet transmission was evaluated in 1.3.3.1. This section extends the evaluation to HTTP and FTP. If NumInterlaces number of interlaces are assigned to one user, the effect on the application delay may be computed as follows.

For an average transmitted packet, Table 1-4 shows that errors cause an average of 0.83 ms extra transmission delay. Consider a file with N bits that is transmitted with a mean packet size of MeanPacketSize. Then, the number of packets transmitted on one interlace is approximately N/(MeanPacketSize*NumInterlaces), and the extra delay incurred in transmission is 0.83*N/(MeanPacketSize*NumInterlaces) milliseconds.

From the description of the traffic model, it is known that the mean transaction size for FTP is 2Mbytes, while for HTTP it is 54 kbytes. Further, from the system simulation, the mean MAC packet size was determined for different loads. This allows the computation of the additional delay for a transaction of mean size. It is assumed that the bulk nature of FTP and HTTP causes NumInterlaces to take the value 6.

Table 1-5 Effect of Signaling errors on application delay under varying load

Load	Mean MAC Packet Size (bytes)		Additional Delay (seconds)	
	HTTP	FTP	HTTP	FTP
20	701	911	0.010	0.30
40	401	487	0.018	0.57
60	206	165	0.036	1.6
80	110	123	0.067	2.2
100	98	134	0.076	2.0
120	140	139	0.053	1.9
140	123	162	0.060	1.7

Comparing the above delay numbers with the delays shown in Figure 1-2 shows that the relative effect of signaling error induced delays on overall application delay is small.

1.4.2 Served Mobile Throughput According to Load

When transfer latency for a traffic model increases drastically, the served throughput for that model also falls as shown in Figure 1-3. At 100-120 users, in the previous diagram, latency increases as FTP throughput falls rapidly towards zero bps. In Figure 1-3, it is obvious that BE workloads (FTP and HTTP) are shed before AF workloads (NRTV) which is itself shed before EF workloads (Voice).

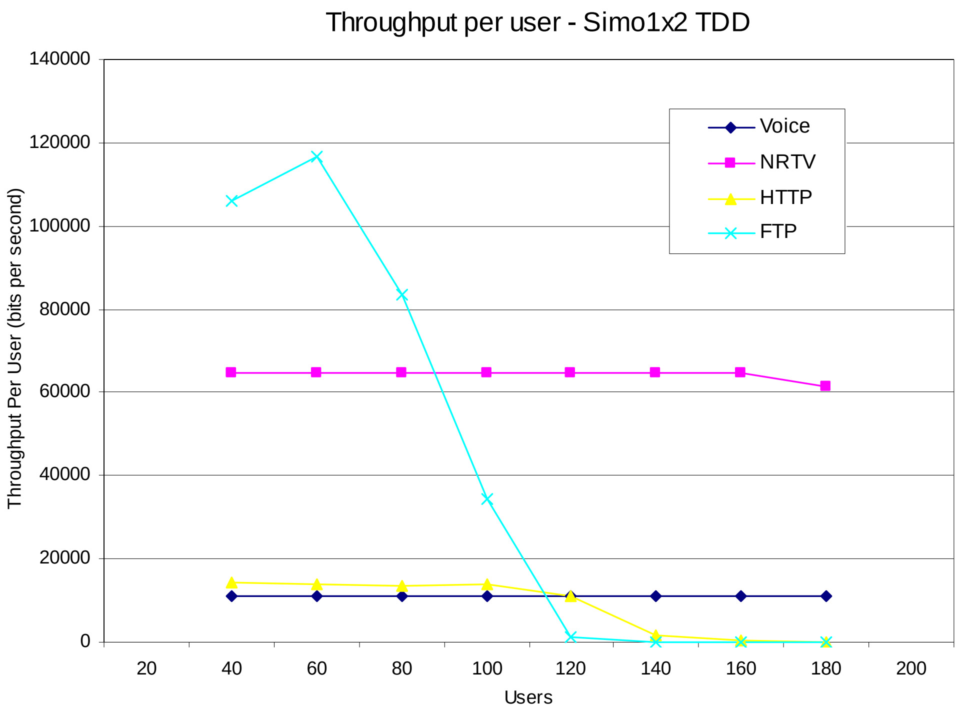

Figure 1-3 Average served throughput per user as a function of load for 30-30-30-10% traffic mix

1.4.3 Mean Download Speed According to Load

Figure 1-4 demonstrates scheduler QoS enforcement as system load increases. In this graph, there is one curve for each flow (VOIP, NRTV, HTTP, FTP), and the x-axis indicates the number of total users/flows per sector. The metric that we graph is the "perceived download speed" once a transfer begins (this is not application throughput, but rather, throughput once a request is made.) Note that while the download speed is a good performance metric for HTTP and FTP flows, download speed beyond the required data rate does not indicate higher level of quality of service for VOIP and NRTV flows. As the workload increases from 40 flows to 180 flows per sector, the highest priority flows see no loss in performance, and the lowest priority flows are gradually starved out of the system. More specifically, the FTP and HTTP flows enjoys high throughput when the system is lightly loaded.

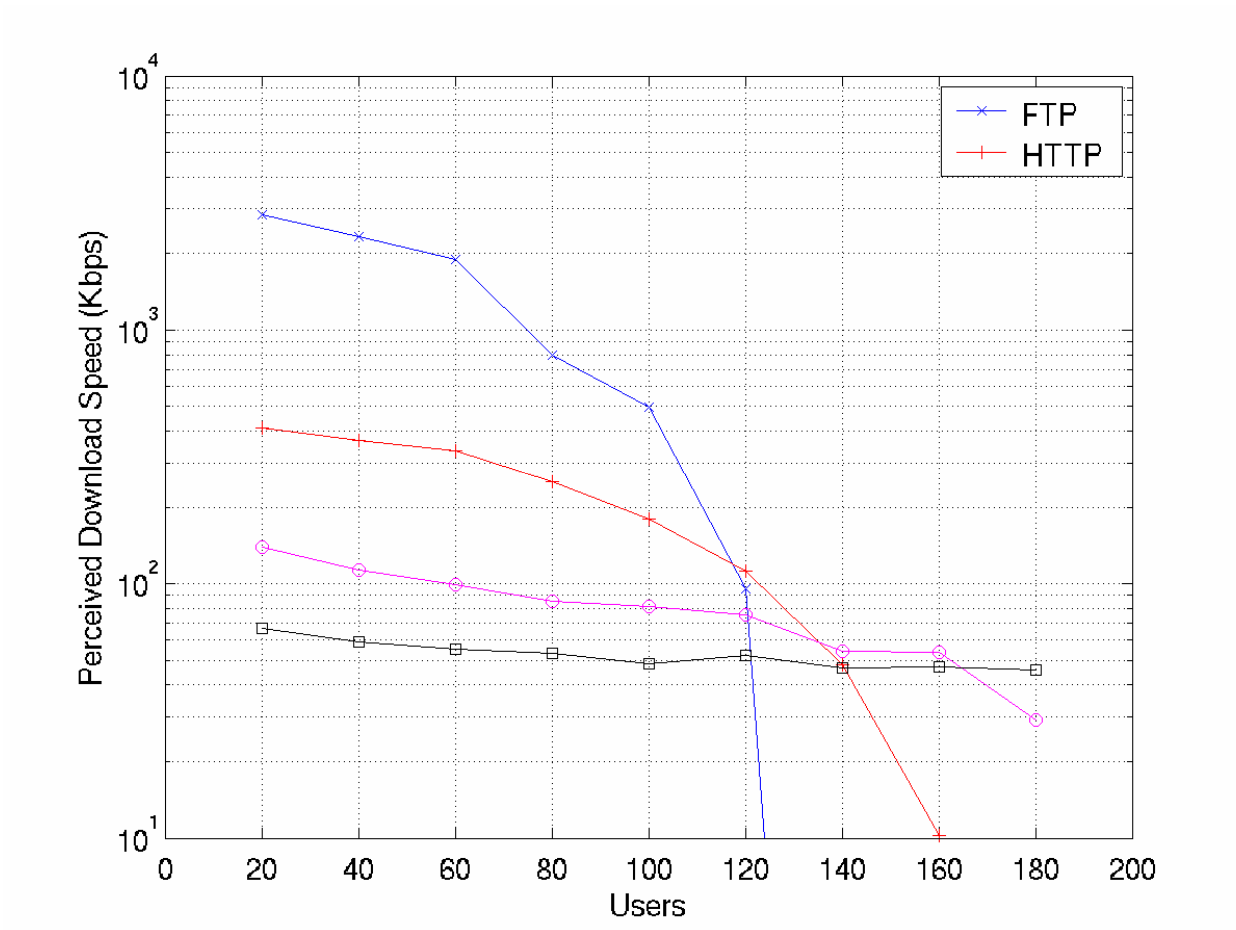

Figure 1-4 Mobile perceived download speed as a function of load, 30 30 30 10% loading, 1 Tx 2 Rx

1.4.4 Voice Performance According to Load

Average and maximum user voice packet error rates were collected as the system load increases. Both the average PER and the maximum packet error rate were collected. The error rate never exceeds 2%, even when 200 users were in the system, as depicted in Figure 1-5.

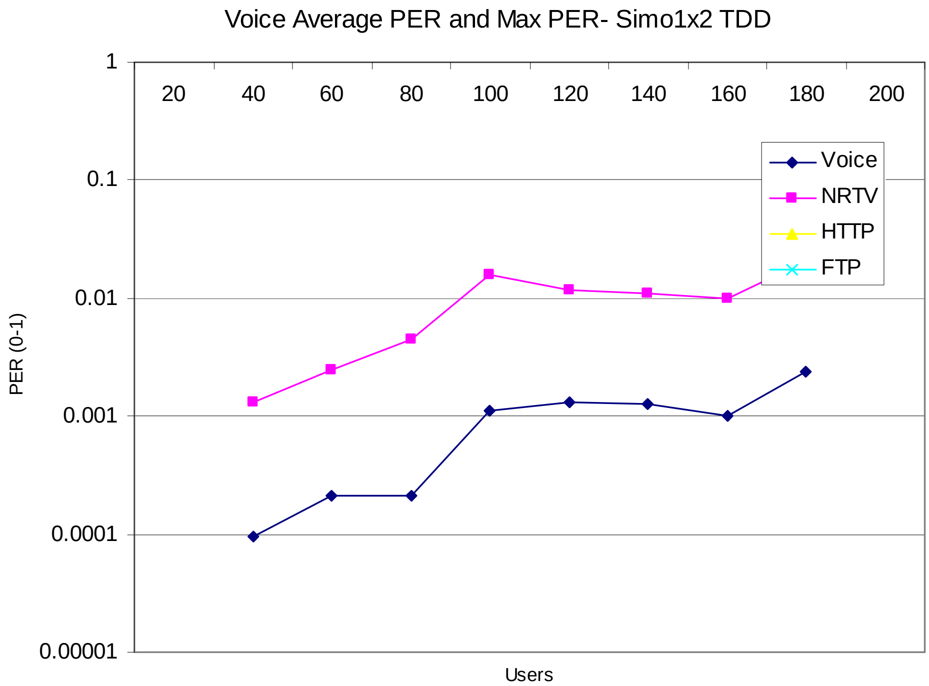

Figure 1-5 Voice PER (average and maximum), 30-30-30-10 mix

1.4.5 Fairness in the Best-Effort Service Class

In 1.4.3, we found that the Best-Effort service class was starved for service at a sector load of roughly 160 users. In Figure 1-6, we report on the fairness for HTTP and FTP at 80 users per sector. It can be seen that the fairness criteria in [1] are met, even as the system carries a heavy QoS load and several other types of traffic.

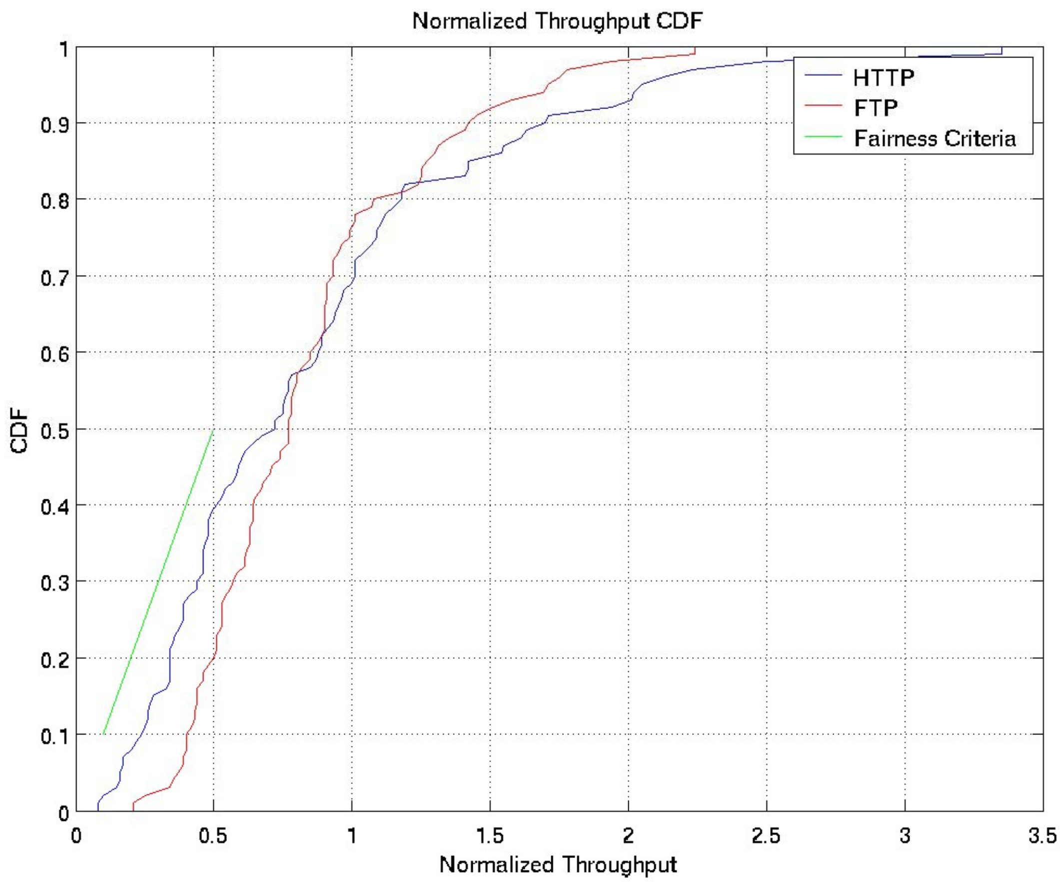

Figure 1-6 Fairness for FTP and HTTP users in 80 users setup

1.4.6 Voice Performance

1.4.6.1 FL Voice Latency Distribution

Figure 1-7 shows the FL voice latency distribution among users of the same class.

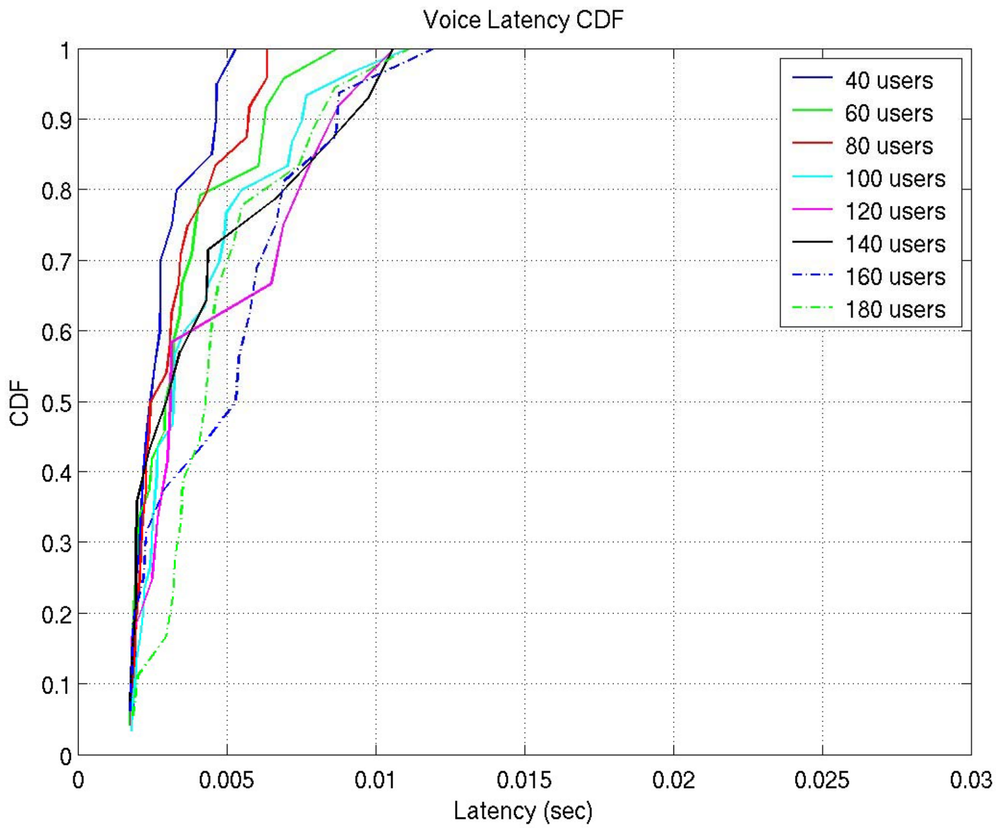

Figure 1-7 Voice Latencies for different number of simo 1x2 users

1.4.6.2 FL Voice E-Model Score Distribution

The G.107 E-Model formula [9] was used to calculate voice quality for the 30-30-30-10 sector loading mix. The results were sorted and are presented in Figure 1-8. Voice quality tends to degrade because of users in poor channel conditions that experience packet loss, not because of latency.

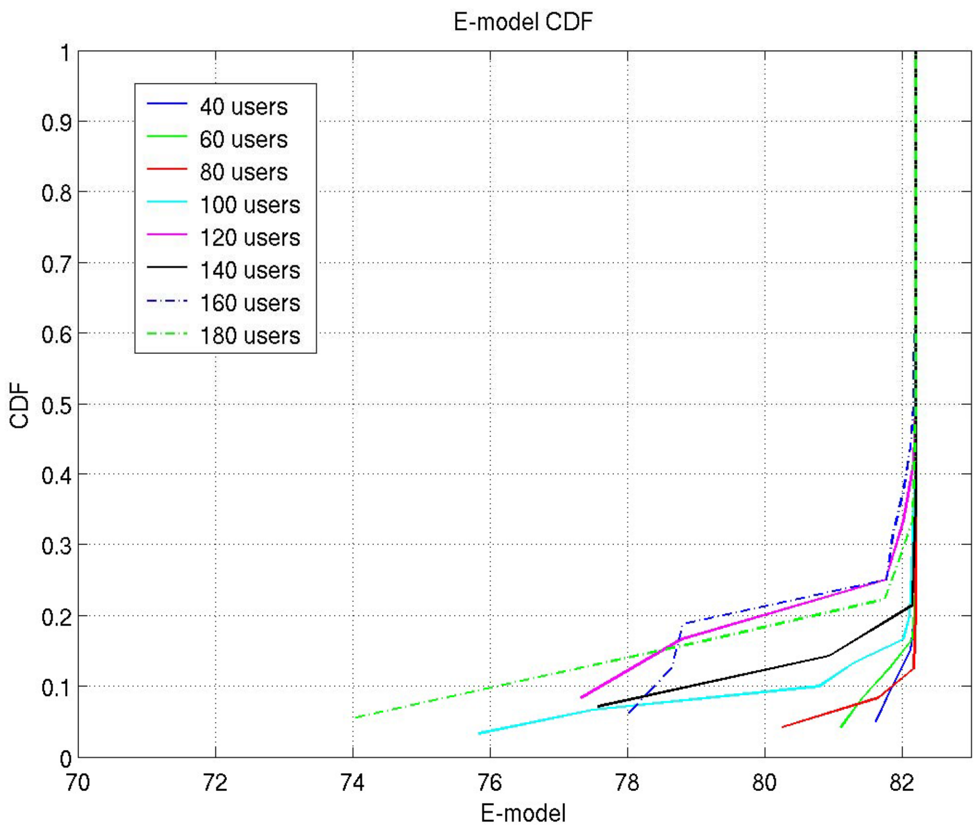

Figure 1-8 Voice E-Model scores voice users, 30-30-30-10 mix, 20-180 users per sector

1.4.7 NRTV Outage

At 180 users, system is just at the capacity level for NRTV and VOIP traffic. Figure 1-9 presents the latency for the worst stream in a simulation of 305 seconds. This was the only streams to exceed a 4-second delay. The maximum packet latency is reported for each 1-second interval. It is apparent that the stream is experiencing 2-3 second delays in packet delivery, over the air interface, and this stream sees a latency higher than 5 second only at a specific second.

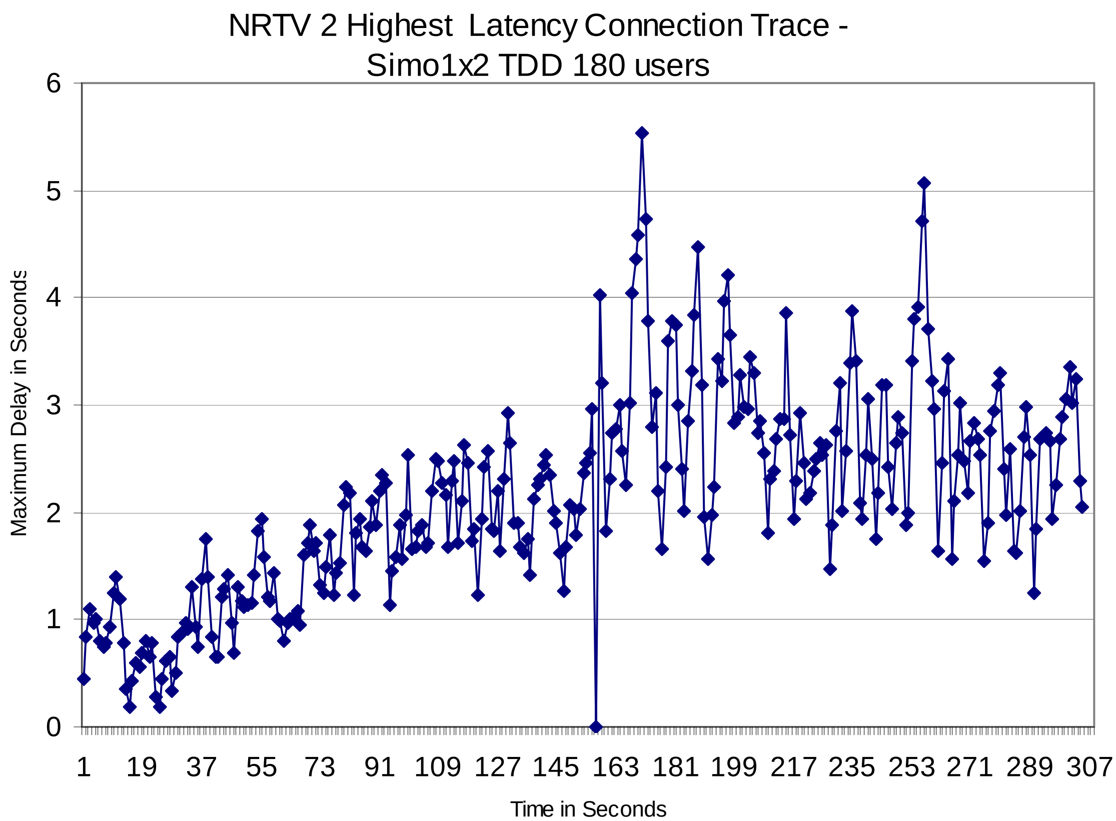

Figure 1-9 NRTV Latency, 2 worst-case streams (of 55), 30-30-30-10 mix, 160 users per sector

1.5 Link Simulation Results for High Mobility

The channel mixes required by the Evaluation Criteria do not include 250 km/h channels in suburban macro mix and 120 km/h channels in urban micro mix. The link level performance under the high speed channels are evaluated in this section.

1.5.1 Forward Link Mobility Simulations

Link level simulations were carried out over different multipath profiles, Doppler spreads, and correlation models. The following simulations assume a 4x4 MIMO single codeword (SCW) design with MMSE receiver. Note that the spectral efficiency is obtained by running link simulations with adaptive rate and rank prediction, channel estimation, and HARQ with 6 maximum retransmissions. A large number of packets are simulated for each fixed geometry, i.e., long term average C/I per antenna. The packet format and rank for each packet transmission are selected based on the latest channel observations. If AT fails decoding, incremental redundancy subpackets will be transmitted until the packet decodes successfully or the maximum transmission is reached. The spectral efficiency computation takes into account the pilot overhead and residual packet errors.

The spectral efficiency curves based on the SCM suburban macro model is illustrated in Figure 1-10. It was observed that the spectral efficiency degrades gracefully as the mobility increases from 3 km/h to 250 km/h, where the highest spectral efficiency achieved at 250 km/h is greater than 7 bps/Hz. The MIMO spectral efficiency based on the SCM urban micro model at 120 km/h is illustrated in Figure 1-11. It is observed that at the geometry of 25 dB, spectral efficiency of 11 bps/Hz and 10 bps/Hz can be achieved for VehA and PedA channel at 120km/h, respectively. For VehB channel the highest spectral efficiency achievable at 120 km/h is greater than 5 bps/Hz.

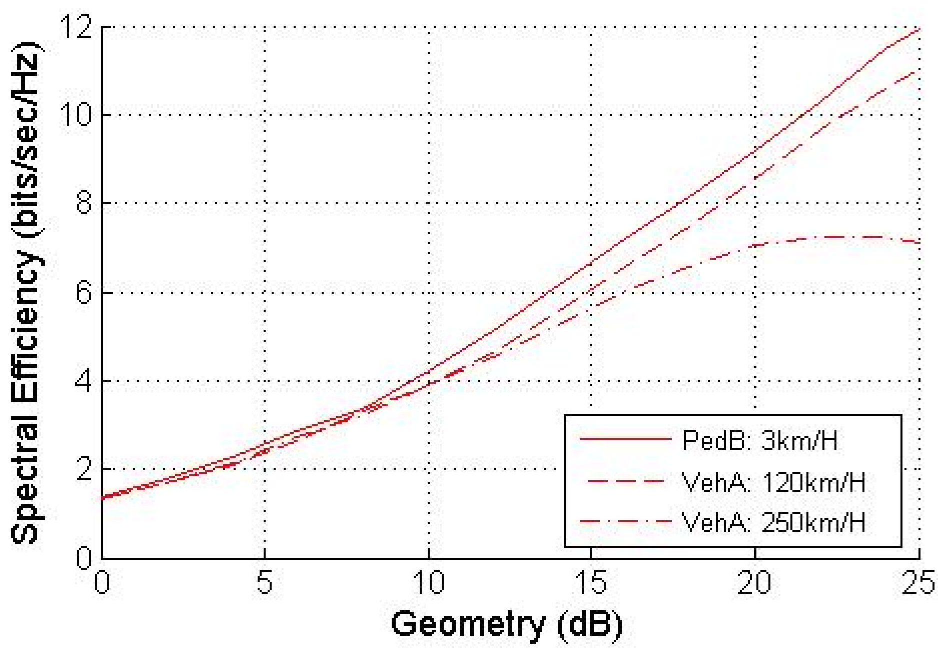

Figure 1-10 Spectral efficiency vs. SINR SCW-MIMO 4x4 with SCM suburban macro cell correlation model. Base station AoD 50 degree, AS 2 degree.

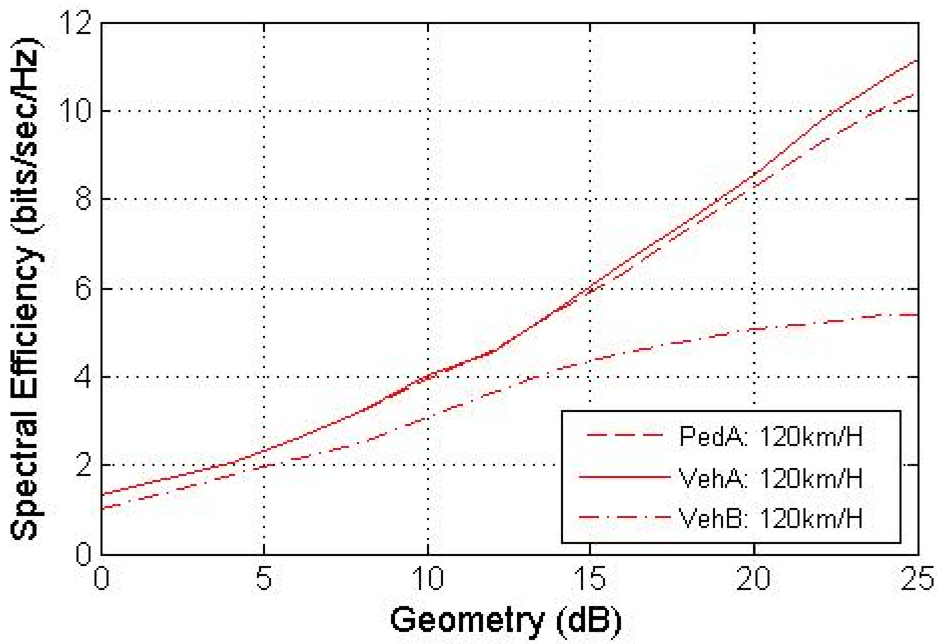

Figure 1-11 Spectral efficiency vs. SINR SCW-MIMO 4x4 with SCM urban micro cell correlation model. Base station AoD 50 degree, AS uniform distribution [-40, 40].

1.5.2 Reverse Link Mobility Simulations

Reverse link mobility sensitivity study results are presented in Figure 1-12 and Figure 1-13. RL packet formats of the desired spectral efficiencies are simulated over a range of SNR, so that an average SNR required to achieve 1% FER is obtained for each packet format. Each point in the plot is the spectral efficiency versus the SNR for the simulated packet format, where 1% packet error is deducted from the final spectral efficiency. Different curves corresponding to five different channel models. The two plots are for 2 and 4 receive antenna, respectively. Note that all link level spectral efficiency results take into account the pilot overheads.

As shown in the following figures, the link level performance degrades gracefully with mobility.

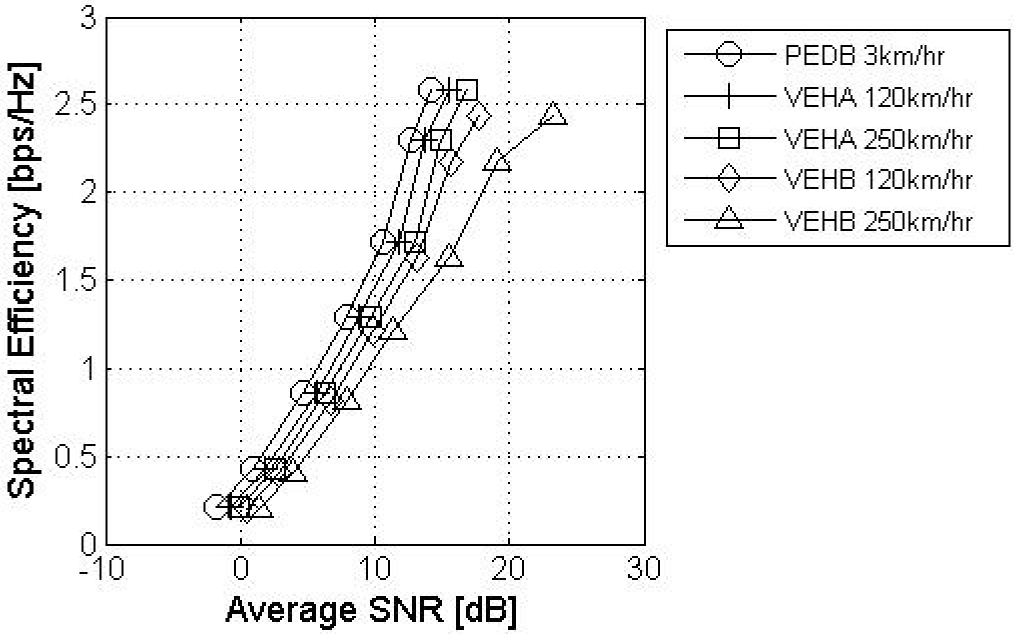

Figure 1-12 Spectral efficiency vs. SINR with dual Rx diversity at BS

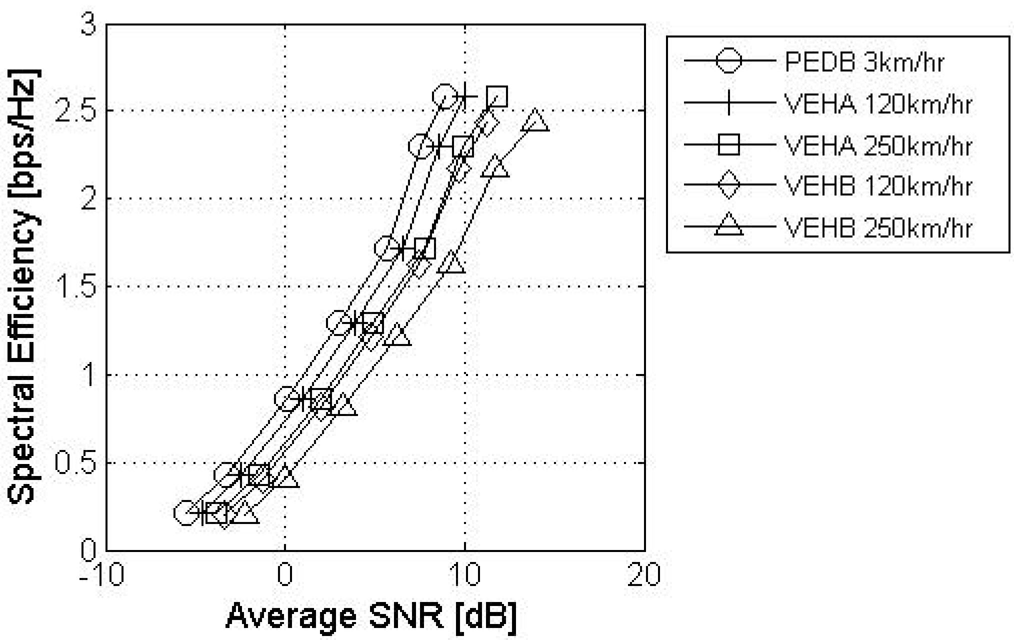

Figure 1-13 Spectral efficiency vs. SINR with 4 Rx diversity at BS

2 Mobility

2.1 Connected State Handoff

In this section, we present the results of mobility and handoff study for the MBWA system. The details of the proposed handoff algorithms are provided in [7]. The call flows of forward link and reverse link handoff in connected state are shown in Figure 2-1 and Figure 2-2. As explained in [7], since the handoff decision is made at the AT, and the indication is sent to the desired serving sector, the current serving sector can continue to serve the AT until the handoff indication is received at the AN, and even during some part of L2 handoff negotiations. As a result, in the proposed design the only outage period, as defined in [1], can happen during the L2 handoff negotiation. For forward link handoff between sectors not belonging to the same cell, this outage period is equal to the amount of time required to transfer the forward looking state to the new sector, i.e., a one-way backhaul delay. For reverse link handoff, and also for forward link handoff between sectors within one cell, this outage period can be significantly smaller.

.

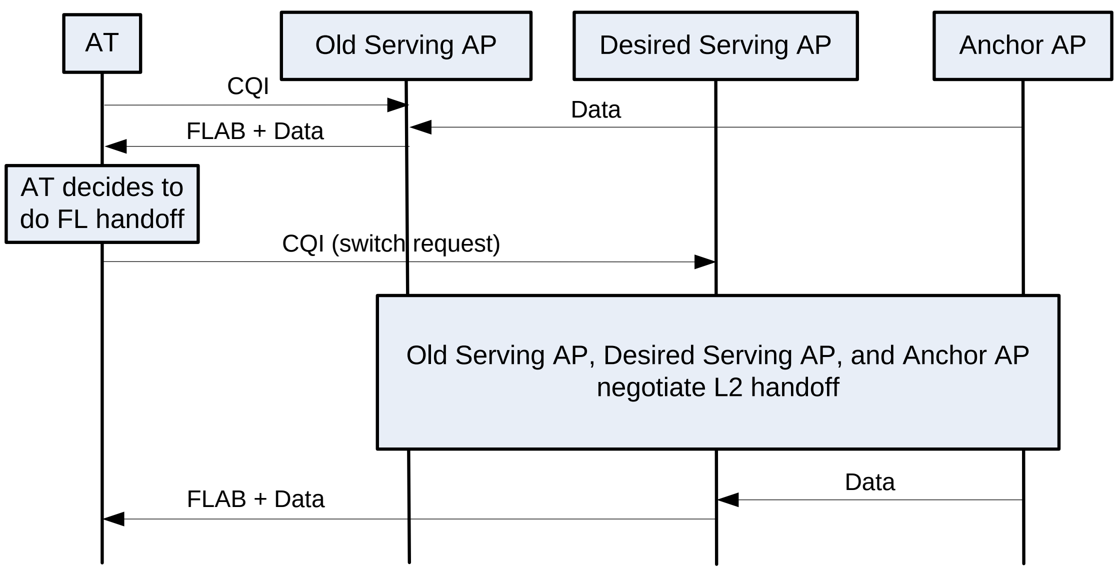

Figure 2-1 Forward link handoff call flow

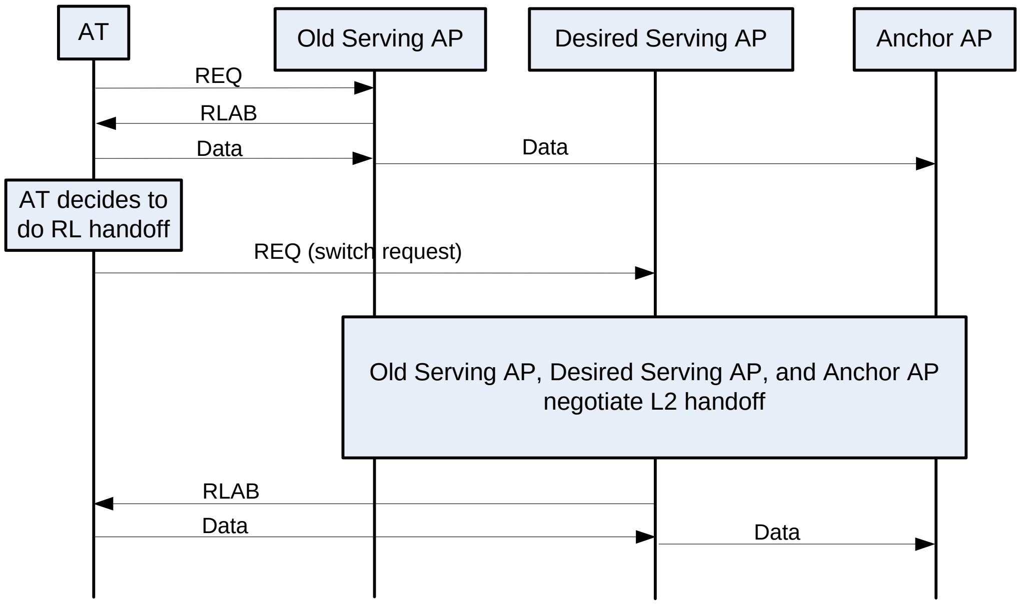

Figure 2-2 Reverse link handoff call flow

Figure 2-3 shows the CCDF of the FL handoff outage period using a shifted Gamma distribution for the backhaul delay with the scale, shape and shift parameters provided in [1] (1, 2.5, and 7.5msec). With these parameters, the average outage period (average one-way backhaul delay) is 10msec. As mentioned, for reverse link handoff, and for forward link handoff between sectors within one cell, this outage period can be significantly smaller.

A connection drop is defined in [1] to occur when the outage period on the uplink or downlink crosses a threshold. From Figure 2-3, we can see that for the thresholds considered in the proposed system specification (which are in the order of a second), the probability of connection drop during handoff is practically zero.

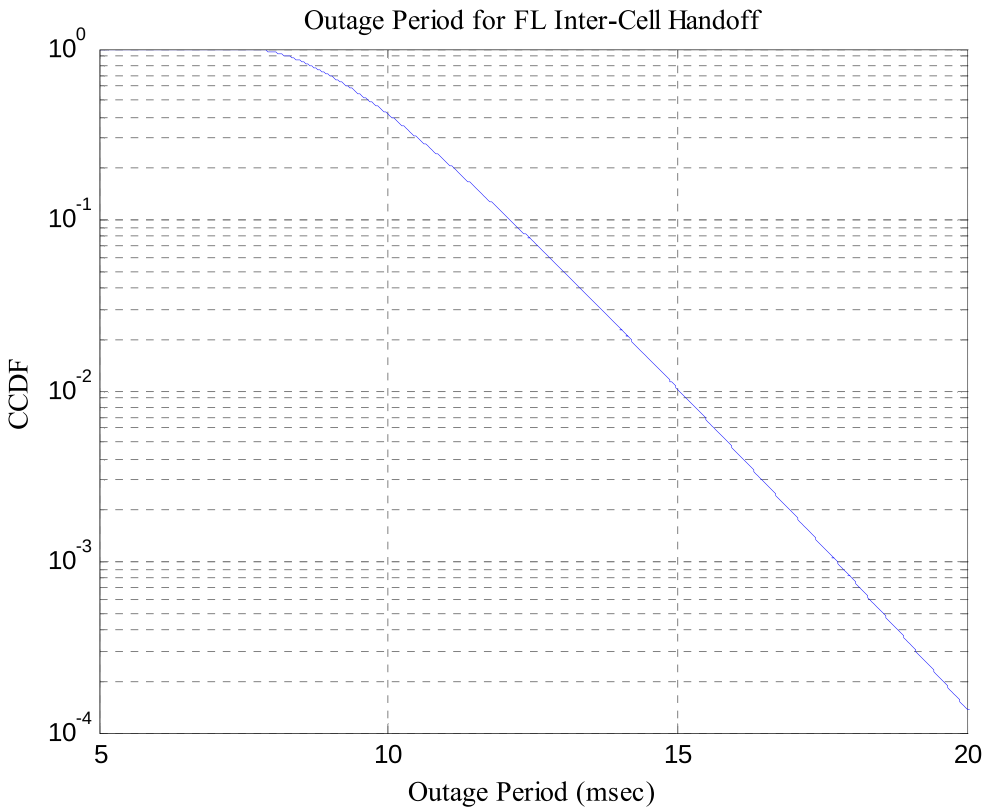

Figure 2-3 Outage period for forward link inter-cell handoff

Next, we provide detailed simulation results and SNR traces for the forward and reverse link handoff using the three mobility models specified in [1]. All terminals except one are fixed. The mobility related performance metrics are computed only for this mobile terminal. The paths corresponding to the three mobility models are shown in Figure 2-4.

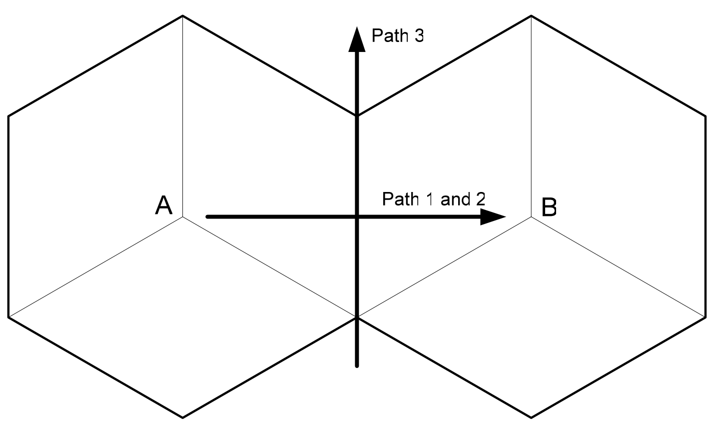

Figure 2-4 The three paths corresponding to the three mobility models

In all cases, we consider a 19 cell layout with wrap around model as specified in [1]. As a reference, we show the inner 19 cells of this layout in Figure 2-5. The legends of the figures in the rest of this section will refer to sector numbers as shown in this figure. The cells A and B in Figure 2-4 correspond to the cells 0 and 1 in Figure 2-5.

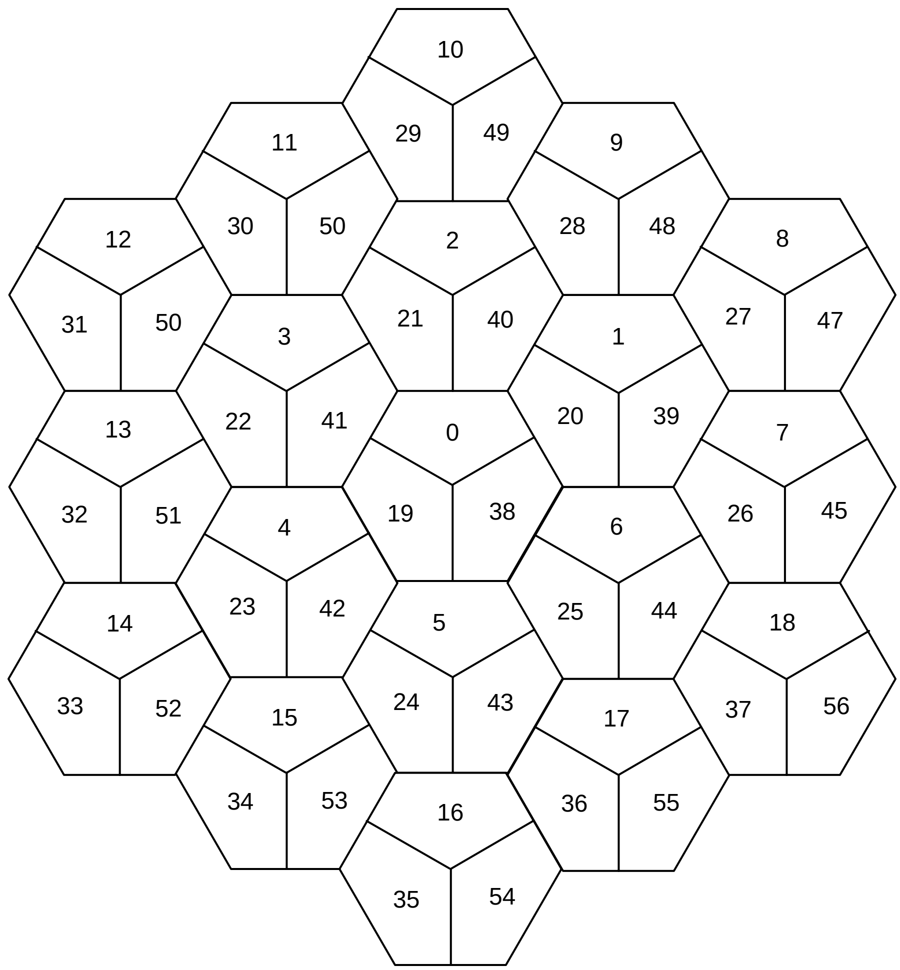

Figure 2-5 The inner 19 cells of the considered wrap around layout

Other parameters of the system simulations are given in Table 2-1.

Table 2-1 Parameters for the Mobility Model

Parameter Name	Interpretation	Value
R	Distance between A and B	1000 m
EdgeLoss	Sudden propagation loss at cell edge for model 2	3, 6, 9 dB
V	Mobile Speed	3, 30, 120 Km/h
D_{corr}	Shadow Fading Corr. Distance	30 m
D_0	Distance of starting point from A in paths 1 and 2 (same as distance of ending point from B)	30 m
D_3	Total distance covered by terminal in path 3	1000 m
FilterTimeConstant	SINR and C/I filter time constant for active set management and handoff decision	100 msec
AddThreshold	Active set add threshold (on filtered SINR)	-7 dB
DropThreshold	Active set drop threshold (on filtered SINR)	-9 dB
DropTimer	Active set drop timer (if the SINR of an active set sector remains below DropThreshold for this period, it is dropped from the active set.)	2 sec
FLHandoffHysteresis	Forward link handoff hysteresis (on filtered effective C/I)	2 dB
RLHandoffHysteresis	Reverse link handoff hysteresis (on CQI erasure indicator rate)	0.1

2.1.1 Mobility Model 1

The mobility path of the non-stationary terminal in model 1 is shown in Figure 2-6. The path starts at a point in cell 0 (on the boundaries of sectors 0 and 38), at a 30m distance from the center of the cell, and ends at point in cell 1 (sector 20), at the same distance from the cell center.

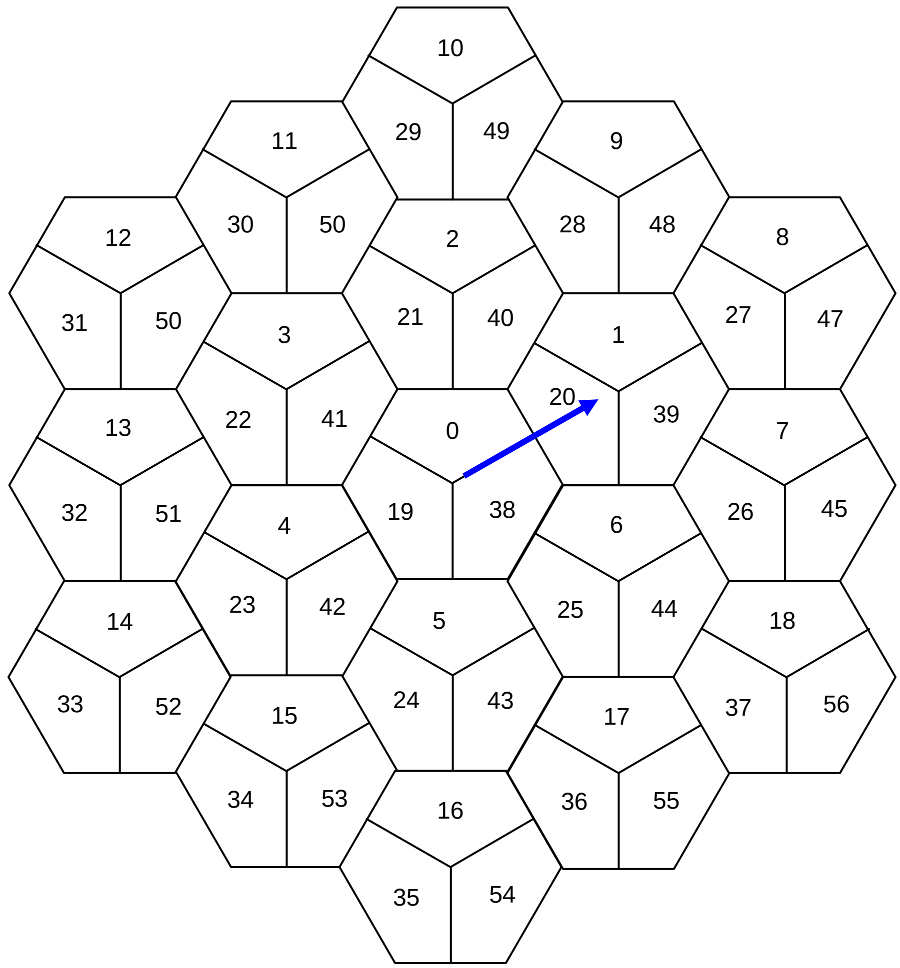

Figure 2-6 The mobility path for the non-stationary terminal in models 1 and 2

Figure 2-7 shows the filtered SINR (geometry) traces for active set sectors of the non-stationary terminal in model 1, with a mobile speed of 120Km/h (Vehicular B channel model). As we see, in the beginning of the path, sectors 0 and 38 belong to the active set (and have the same SINR values, since the terminal has the same path loss, shadow fade, and antenna gain to both of them). As the terminal moves along the path, new sectors get added to the active set, or some of the existing sectors get dropped from the active set. The vertical green line shows the instance at which the terminal crosses the boundary of cell 0 and enters cell 1.

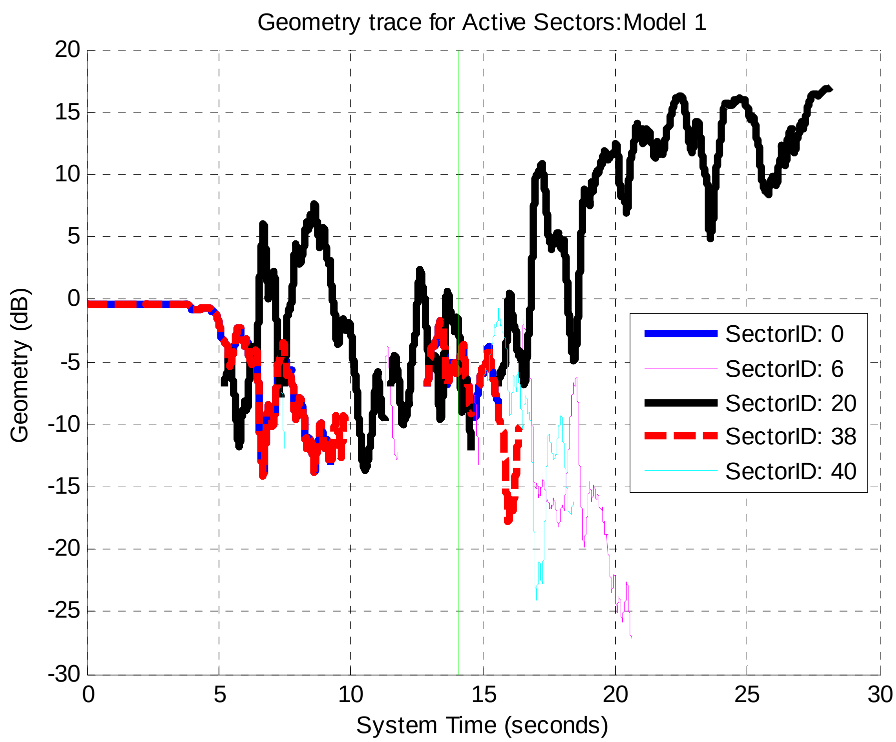

Figure 2-7 Geometry traces for active set sectors, model 1

2.1.2 Mobility Model 2

The mobility path of the non-stationary terminal in model 2 is similar to model 1, and is shown in Figure 2-6. The difference between model 2 and model 1 is in the additional edge loss parameter. Three values of 3dB, 6dB, and 9dB are considered for the edge loss.

2.1.2.1 3dB Edge Loss

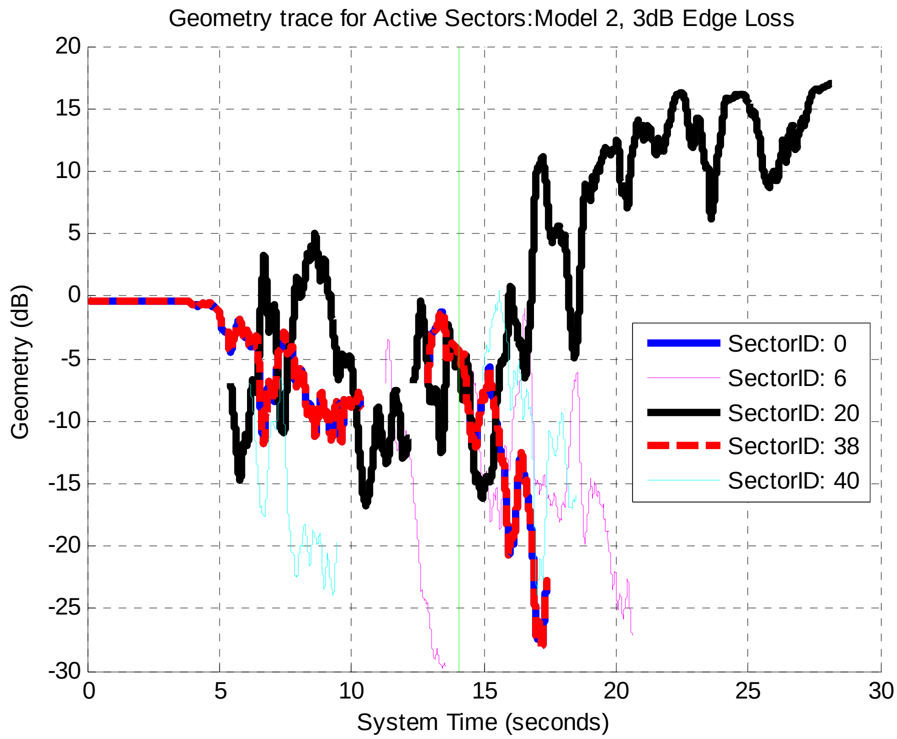

Figure 2-8 Geometry traces for active set sectors, model 2 with 3dB edge loss

Figure 2-9 shows the traces of filtered effective C/I values for active set sectors for some part of the mobile path. The mobile speed is assumed to be 120Km/h (Vehicular B channel model). The vertical lines mark the handoff events. The serving sector of the mobile in each region is also shown on the figure.

Figure 2-10 shows similar traces for mobile speed of 30Km/h (Vehicular B channel model).

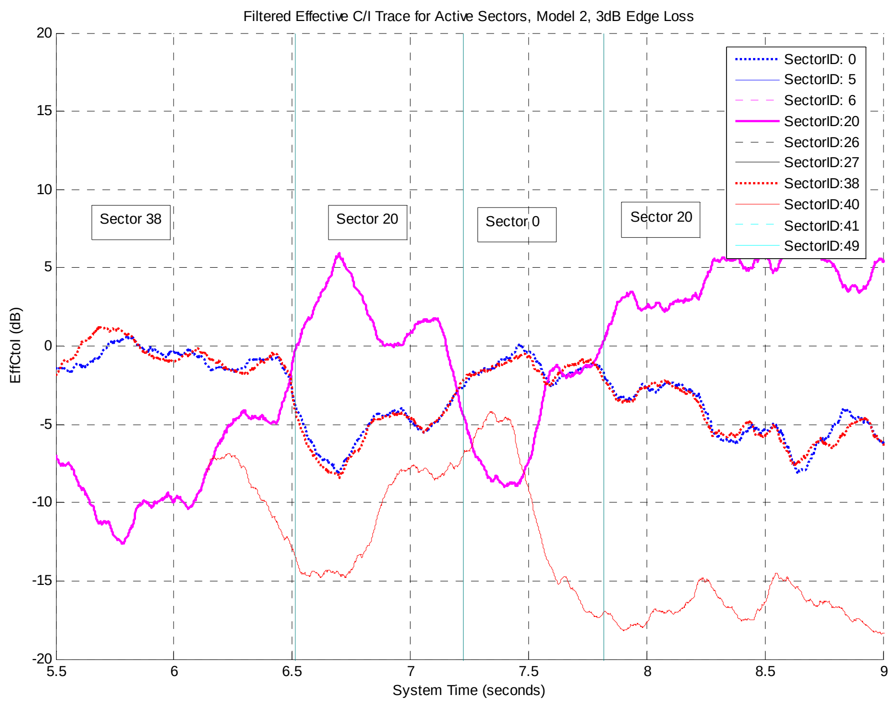

Figure 2-9 Traces of filtered effective C/I for model 2 with 3dB edge loss and mobile speed of 120 Km/h

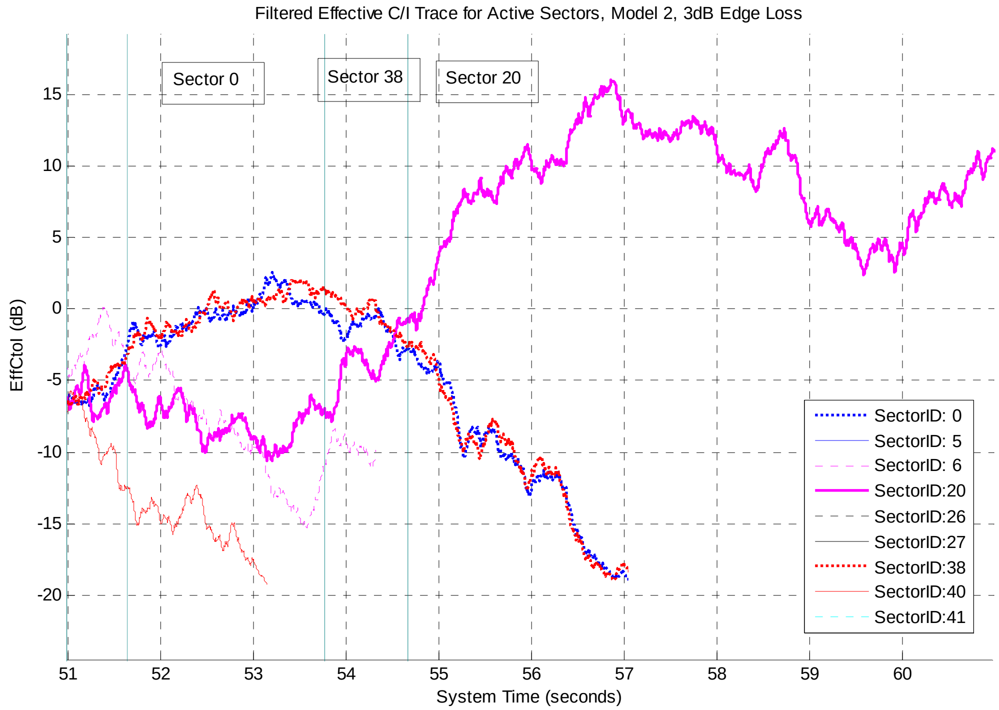

Figure 2-10 Traces of filtered effective C/I for model 2 with 3dB edge loss and mobile speed of 30 Km/h

2.1.2.2 6dB Edge Loss

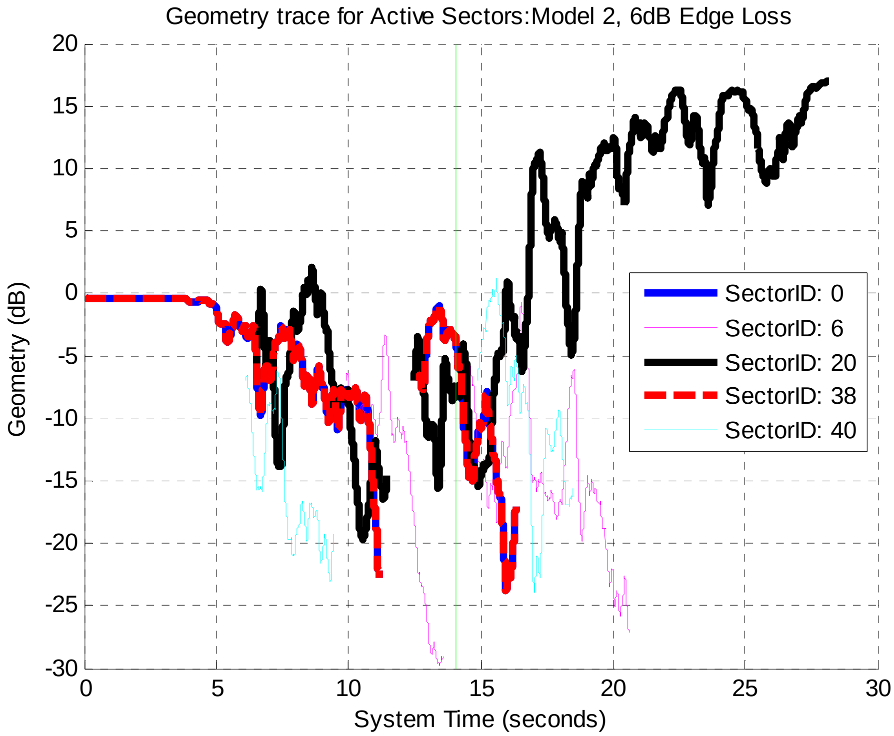

Figure 2-11 Geometry traces for active set sectors, model 2 with 6dB edge loss

Figure 2-12 shows the traces of filtered effective C/I values for active set sectors for some part of the mobile path. The mobile speed is assumed to be 3Km/h (Pedestrian B channel model).

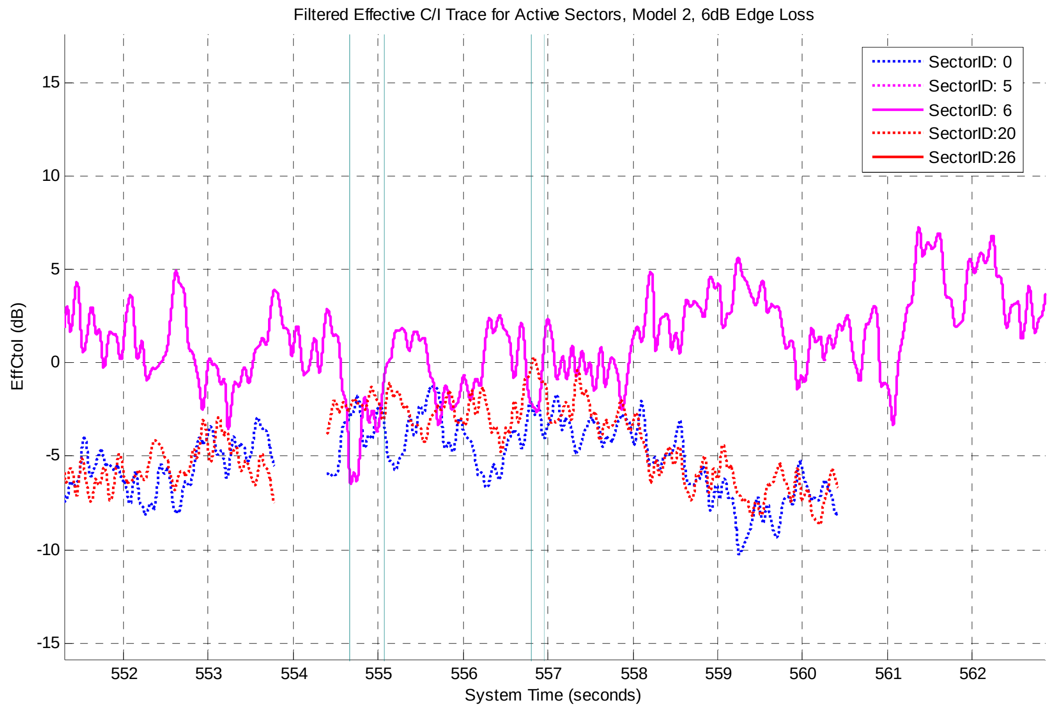

Figure 2-12 Traces of filtered effective C/I for model 2 with 6dB edge loss and mobile speed of 3 Km/h

2.1.2.3 9dB Edge Loss

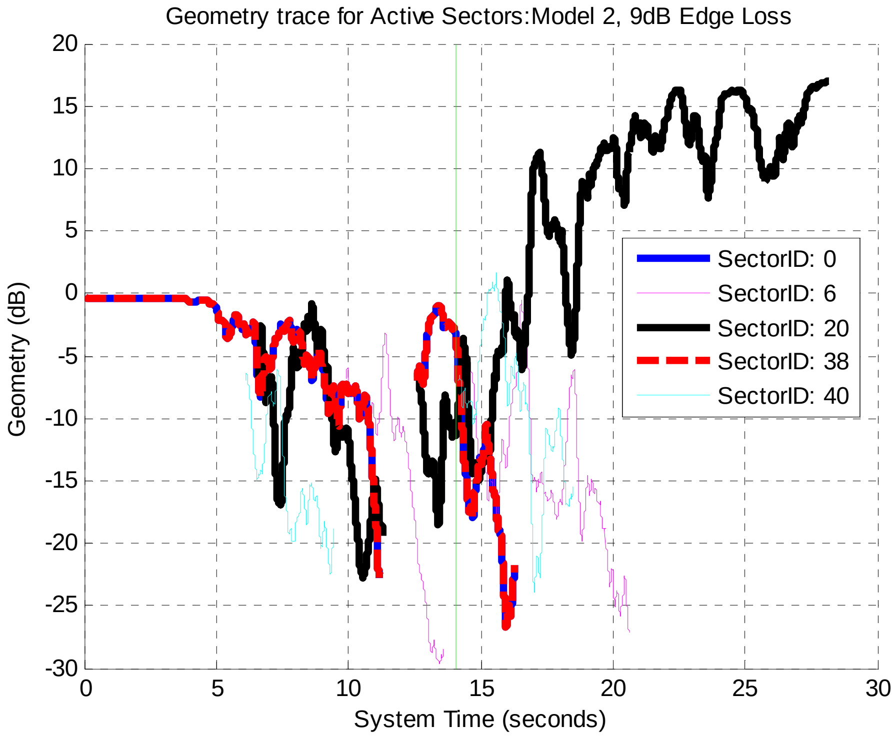

Figure 2-13 Geometry traces for active set sectors, model 2 with 9dB edge loss

2.1.3 Mobility Model 3

The mobility path of the non-stationary terminal in model 3 is shown in Figure 2-14. The path starts at a point in cell 6 (sector 6) and ends at a point in cell 2 (sector 40), and the length of the path is equal to the site-to-site distance, which is assumed to be 1000m.

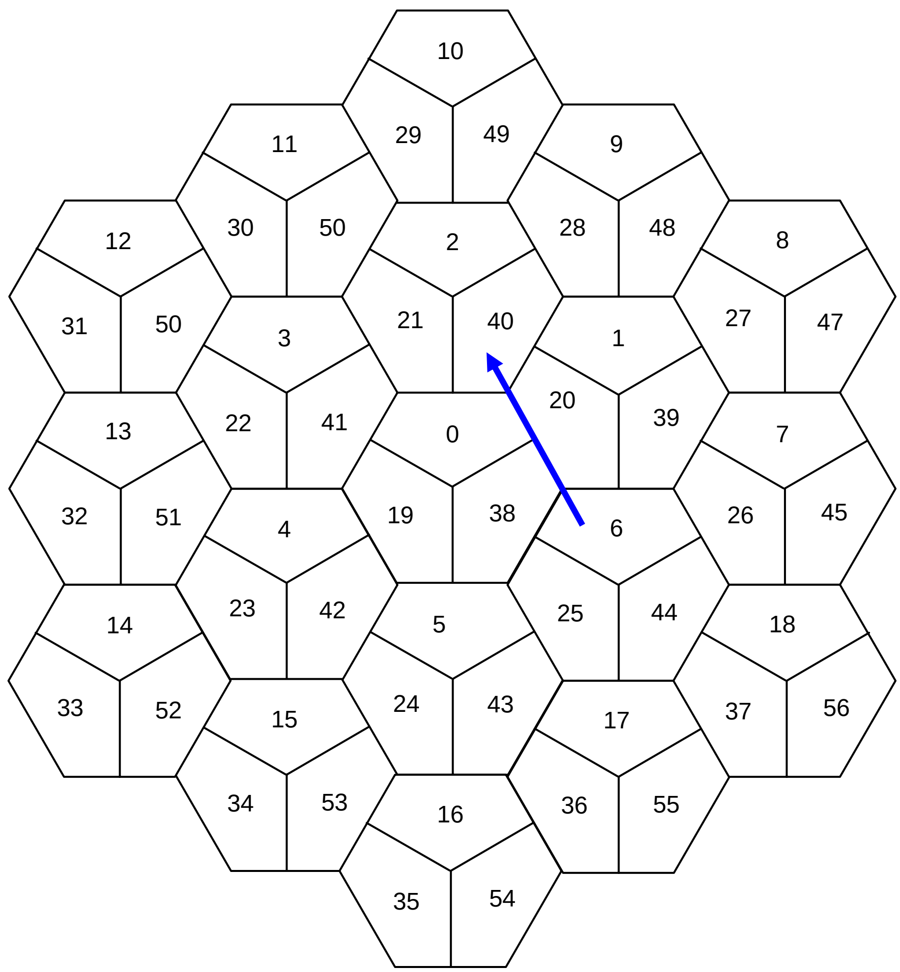

Figure 2-14 The mobility path for the non-stationary terminal in models 3

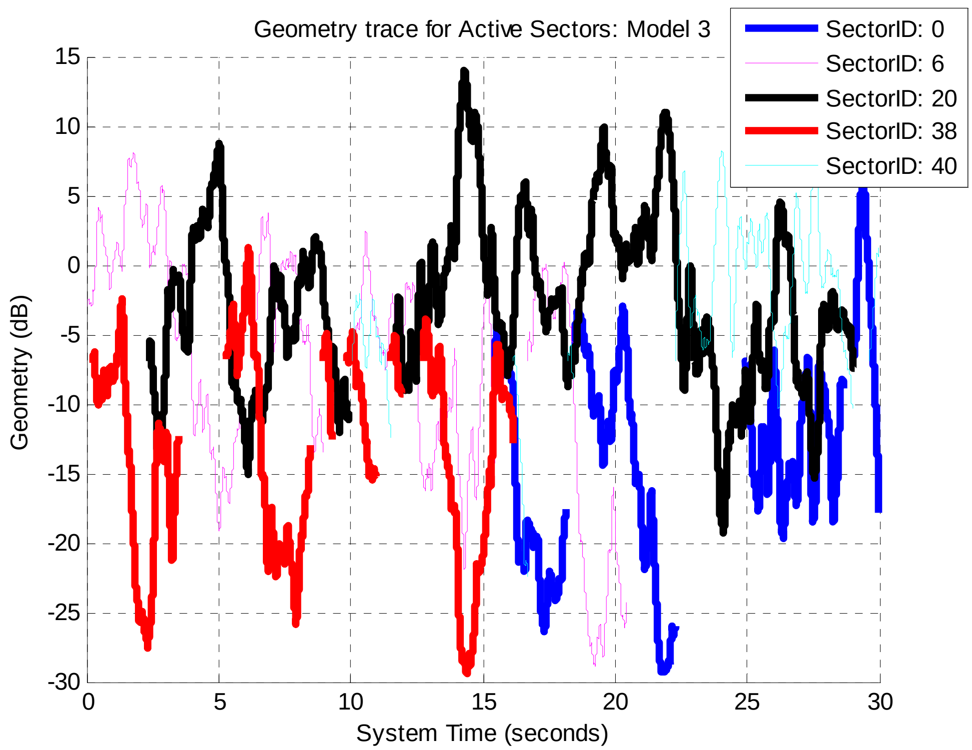

Figure 2-15 Geometry traces for active set sectors, model 3

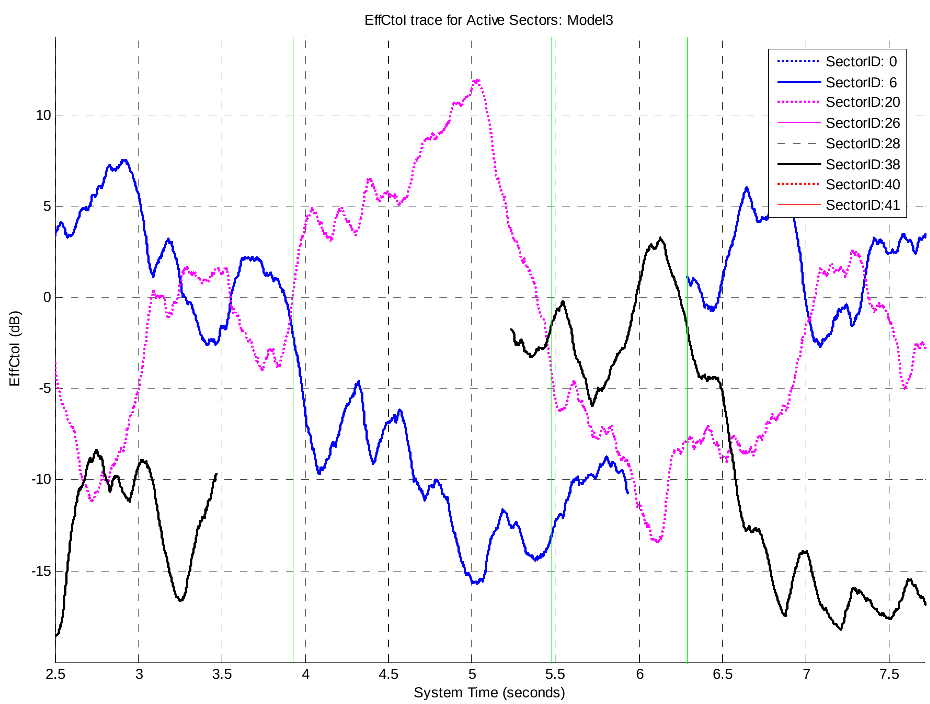

Figure 2-16 Traces of filtered effective C/I for model 3 and mobile speed of 120 Km/h

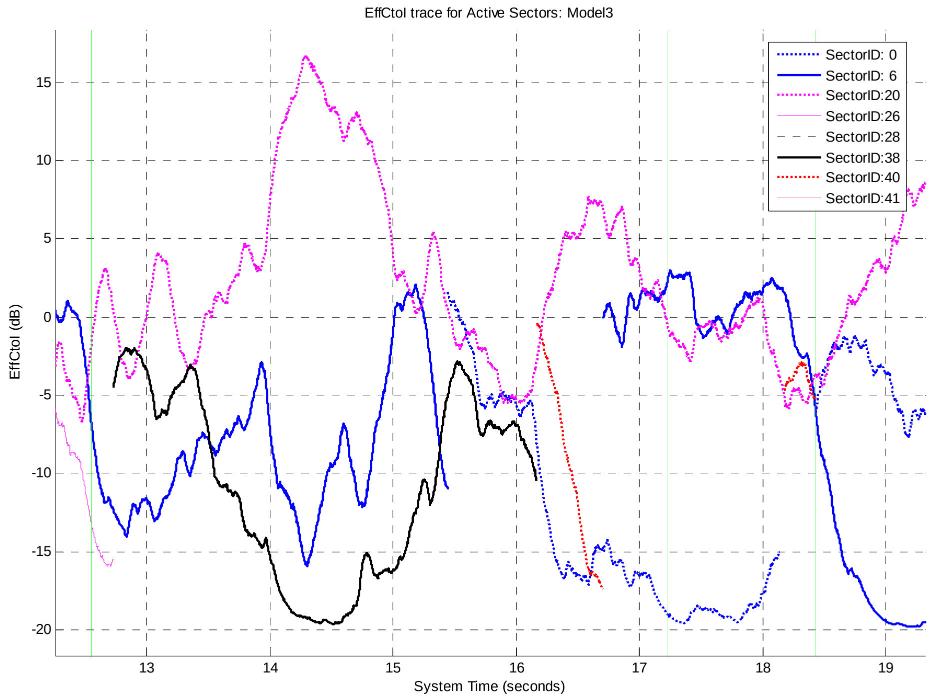

Figure 2-17 Traces of filtered effective C/I for model 3 and mobile speed of 120 Km/h

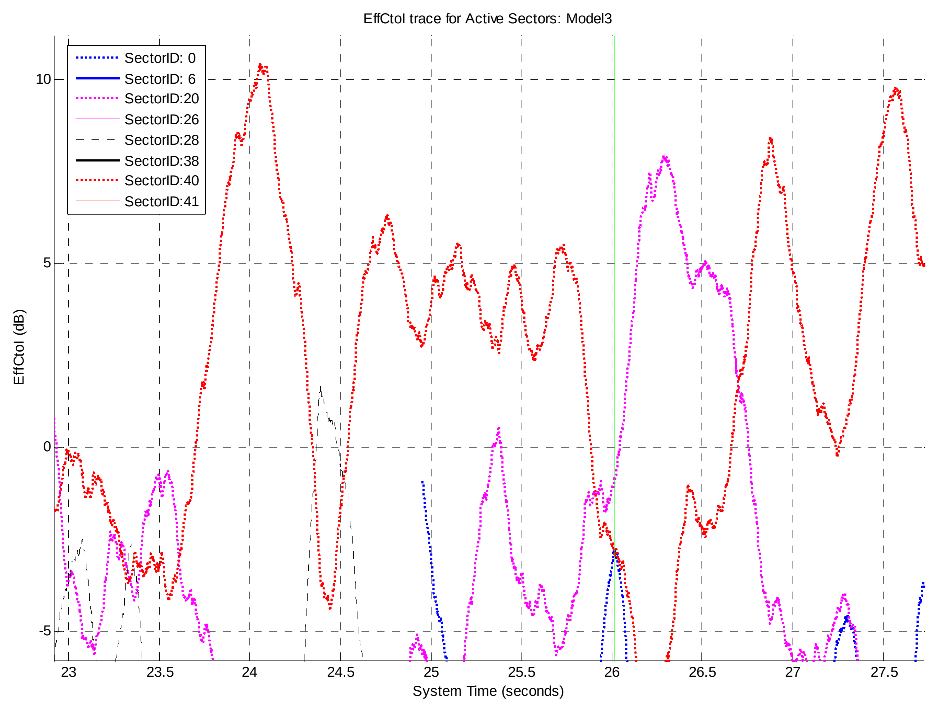

Figure 2-18 Traces of filtered effective C/I for model 3 and mobile speed of 120 Km/h

2.1.4 Handoff Delay Statistics

Figure 2-19 and Figure 2-20 show the CDFs of forward and reverse link handoff delay. This delay is defined as the delay between the handoff decision time (i.e., the time of degradation of serving sector signal relative to the desired serving sector signal) and the handoff completion time (i.e., the time of receiving new assignment from the desired serving sector). It includes the handoff signaling delay, as well as the back haul delay during L2 handoff. Notice that this delay is not equal to the outage period as defined in [1]. The outage may happen only during some part of the L2 handoff negotiations, as explained in 2.1, and the duration of outage is generally much smaller than the handoff delay. Also, the handoff delay distributions are similar for different mobility models and mobile speeds (the handoff decision times can be different, though).

As mentioned earlier, on forward link, inter-cell handoffs may experience a larger delay due to the delays involved in state transfer during L2 handoff. As a result, on forward link, the CDFs and the mean values of inter-cell and intra-cell handoff delays are different, as shown in Figure 2-19. This is not the case for the reverse link, as shown in Figure 2-20.

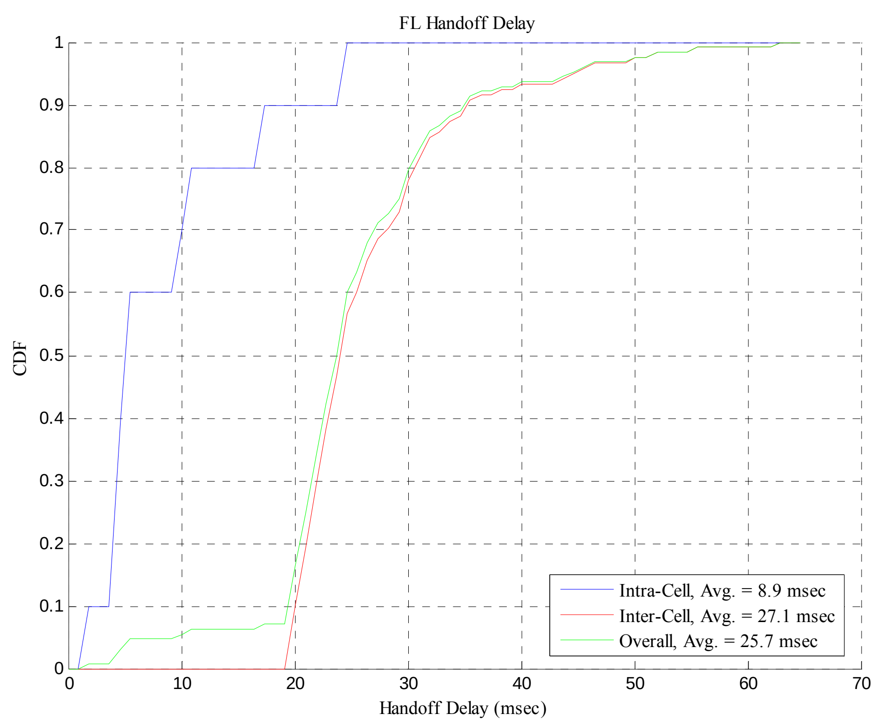

Figure 2-19 Forward link handoff delay CDF

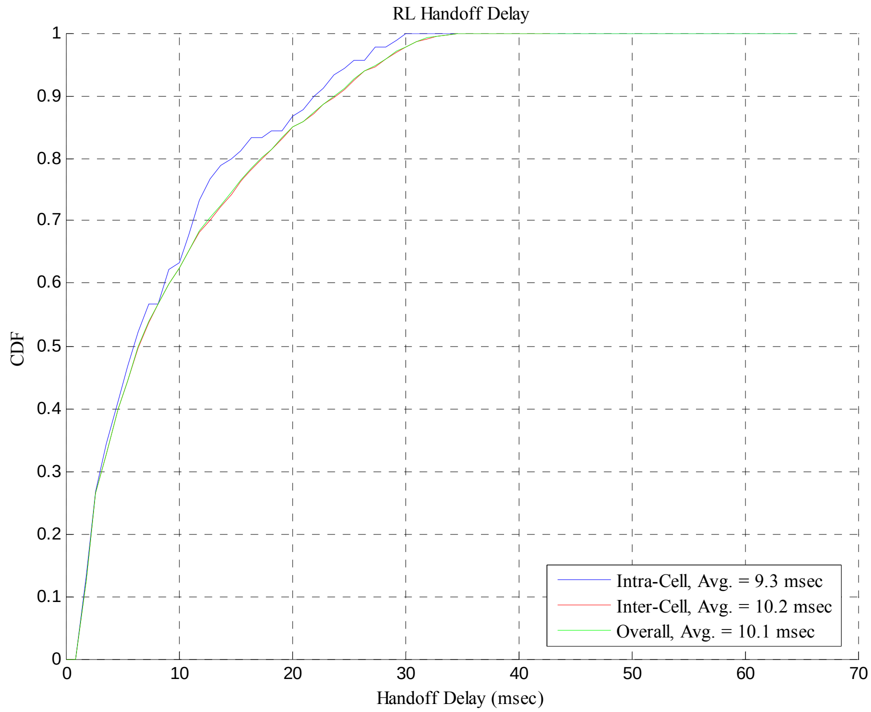

Figure 2-20 Reverse link handoff delay CDF

2.2 Idle State Performance

The proposal supports idle state operation where the terminal checks for pages periodically and may make an access attempt at any time. Operation in idle state is described by the Idle State Protocol in the Lower MAC Control Sublayer [5].

2.2.1 Duty cycle in idle state

The duty cycle is a function of the paging period. Paging periods that are multiples of two superframe durations are supported, and the paging period measured in superframes is denoted by N_{Paging}. In each paging period, the access terminal is required to receive 8 OFDM symbols of the superframe preamble (of these five OFDM symbols contain the QuickPage block, and others may be used for pilot search). The duty cycle of the access terminal is given by (Superframe Preamble Duration)/(N*Superframe Duration).

For TDD (1:1), it may be seen from Section 7 of [7] that the number of symbols in a superframe is 24*8 + 8 = 200, the duration of a superframe preamble is 1.07 ms, and the duration of a superframe is 24.08 ms.

These numbers give the following duty cycles in idle state.

Table 2-2 Duty cycle in idle state (TDD 1:1)

Paging period in superframes	Paging period in seconds	Duty Cycle (%)
2	0.0481	2.2
16	0.385	0.28
32	0.770	0.14
64	1.540	0.069.
128	3.08	0.035

In addition to the above duty cycle, the access terminal is required to maintain current overhead parameters (QuickChannelInfo and ExtendedChannelInfo). However, the relative receiver On Time required to update the overhead parameters is small because the overhead parameters have expiry timers, and do not change often. For example, if the expiry timer is 120 seconds, the access terminal is required to monitor the overhead channel only once every 120 seconds. Further, the overhead channels are transmitted at know times, further reducing the time the access terminal takes to update the overhead parameters.

2.2.2 Delay in transition to Connected State under normal operation

In most cases, the access terminal will attempt to make an access attempt in a sector from which it was monitoring pages (the current sector). In this case, the design of the overhead channels allows the access terminal to make an access attempt with little delay. The access terminal keeps overhead parameters for the current sector up to date at all times by monitoring the overhead channel, and therefore can make an access attempt in the first access opportunity. Since an access opportunity occurs once every six frames (5.5 ms) the access latency is low.

2.2.3 Overhead for Paging

The paging overhead consists of two parts

1. QuickPaging on pBCH1
2. Paging on the traffic channel

The QuickPaging channel is part of the superframe preamble, and constitutes a 1.25% overhead (see 2.2.1).

The traffic channel is used to carry pages only if a superframe carries two or more pages. Pages on the traffic channel are carried as traffic channel packets with broadcast MAC ID. Note that if there is only one page to be delivered, that page may be delivered using just the QuickPaging channel (without using the traffic channel).

In order to calculate the overhead due to paging, we assume a paging load that follows a Poisson arrival with mean of 20 pages/second/sector. This results in an average of approximately 20*0.024=0.48 pages/superframe. Since a QuickPage block occurs every two superframes, the average load is 0.96 pages per QuickPaging block. For a Poisson random variable with mean 0.96, the probability of a value 2 or more is 0.2. Thus, only 20% of QuickPaging cycles require the use of the traffic channel to deliver a page.

A conservative choice for the packet format is PF0 with six HARQ transmissions, resulting in a spectral efficiency of 0.033 bits/sec/Hz. The actual choice of packet format is up to the scheduler and out of scope of the specification. In case a page is to be delivered over the traffic channel, a page to two users requires approximately 96 bits (see details in the Forward Traffic Channel MAC header description in [5]).

A 96 bit packet sent at the said spectral efficiency requires a 64 carrier assignment. Recall that a 64 carrier assignment with six HARQ transmissions includes 64*8*6=3072 modulation symbols, and at a spectral efficiency of 0.033, can carry up to 102 bits. The overhead resulting from this packet can be calculated as 3072 divided by the number of modulation symbols in two superframes. For 5 MHz system bandwidth, this is 2*25*8*512=204800 symbols, giving an overhead of 3072/204800=1.5%. Since only 20% of all QuickPaging cycles require a page transmission on the traffic channel, the overhead is 0.2*1.5% = 0.3%.

Though the overhead for paging may vary across superframes (as allowed by the flexible QuickPaging and paging design), the average overhead for paging, assuming 20 pages/second/sector on a 5MHz system, including the QuickPage and paging over the traffic channel is 1.25+0.3=1.55%.

2.2.4 Error rate for Paging

Conditioned on the access network sending a page to the access terminal, a paging error can occur if one of the following events occurs

1. QuickPaging block error
2. SSCH assignment error
3. Page packet error

The combined probability of these errors is 0.25, as calculated below.

2.2.4.1 QuickPaging block error

The QuickPaging block is in error if the pBCH1 channel is in error. The average error probability is calculated by averaging the pBCH1 error probabilities as a function of SNR with respect to the distribution of SNR’s seen in the system simulation. This averaging gives 0.2% error rate on the pBCH1

2.2.4.2 SSCH assignment error

Since paging related assignments constitute a small fraction of assignments sent over the SSCH, it is assumed that paging related assignments are sent at high enough power to give negligible probability of error.

2.2.4.3 Page packet error on traffic channel

The error probability for a page on the traffic channel is calculated by averaging the traffic channel error probabilities as a function of SNR with respect to the distribution of SNR's seen in the system simulation. This averaging gives a 0.05% error rate.

2.2.4.4 Recovery from paging errors

Though the probability of paging errors is low as shown above, the following technique is used in the proposed system to further improve paging reliability.

Fast Repage: To reduce the effect of paging errors, a Fast Repage technique is available in the proposed system to reduce the probability of a page being missed. The proposed design allows for the Page to be resent in 0.5 seconds using the following rules

1. If the access terminal determines that a paging error has occurred, it wakes up to read a page after 0.5 seconds

2. If the access network does not receive a response to a Page, it resends the page in 0.5 seconds.

2.2.5 Performance with base station reselection

The access terminal wakes up periodically to read Pages. The case when the access terminal wakes up in a new sector is rare for most access terminals. Since reliable page reception is an important system requirement, the proposed system minimizes the probability of a page being missed upon base station reselection, but does not optimize the delay to set up a connection after base station reselection.

2.2.5.1 Probability of missed page upon base station reselection

To minimize the probability of a page being missed, the design incorporates the following two features.

1. The QuickPage block is carried over pBCH1. The pBCH1 channel does not depend on any sector specific parameters, and may be decoded by the access terminal using information contained in a superframe preamble.

2. The Page is carried over the Forward Data Channel (FDCH), and the access terminal can decode the FDCH if it knows the QuickChannelInfo block that is transmitted in every other superframe.

Due to these two features, the access terminal does not miss a page due to lack of knowledge of overhead parameters. The only case that can cause a missed page is an error on the channel on which the Page or QuickPage is carried.

The probability of this failure of pBCH1 is extremely low given the 0.03 spectral efficiency target for pBCH1.

2.2.5.2 Delay in transition to Connected State upon base station reselection

Base station reselection works as follows. The access terminal wakes at the beginning of a preamble to read a page. If the access terminal has moved to a new sector during the paging period, i.e., the superframe preamble is received from a different sector, the access terminal performs the following steps

1. Buffer the entire superframe preamble (including the TDM pilots)

2. Decode pBCH1 and check the QuickPage block. The decoding of pBCH1 may require use of the TDM pilots.

3. Monitor pBCH1 that is broadcast in the superframe preamble of the next superframe. This preamble will contain the QuickChannelInfo block from the new sector.

4. Wait for a worst case of $N_{OMPExtendedChannelInfo}$=16 superframes to receive an ExtendedChannelInfo block.

5. The access terminal is now ready to make an access attempt.

The worst case wait before an access attempt can be made at a new sector is therefore 18 superframes = 0.47 seconds.

3 Performance Enhancements with Advanced Antenna Techniques

3.1 MIMO Multiple Codeword vs. Single Codeword

Multiple codeword (MCW) with successive interference cancellation (SIC) receiver is a capacity archiving scheme for MIMO systems. Therefore, MCW performs better than single codeword design at the expense of high complexity and memory requirement [7]. Figure 3-1 illustrates the spectral efficiency performance of 4x4 MCW and single codeword (SCW) based on the SCM suburban macro model with PedB channel at 3km/H. The effects of rate/rank prediction, HARQ, turbo code, channel and interference estimation error are all captured in the performance results. The antenna setup is 4 transmitter antennas and 4 receiver antennas with 10 λ spacing at the AP and 0.5 λ spacing at the AT. It is observed that at low geometry (up to 5dB), SCW performs similarly to MCW. The gain of MCW over SCW increases with geometry.

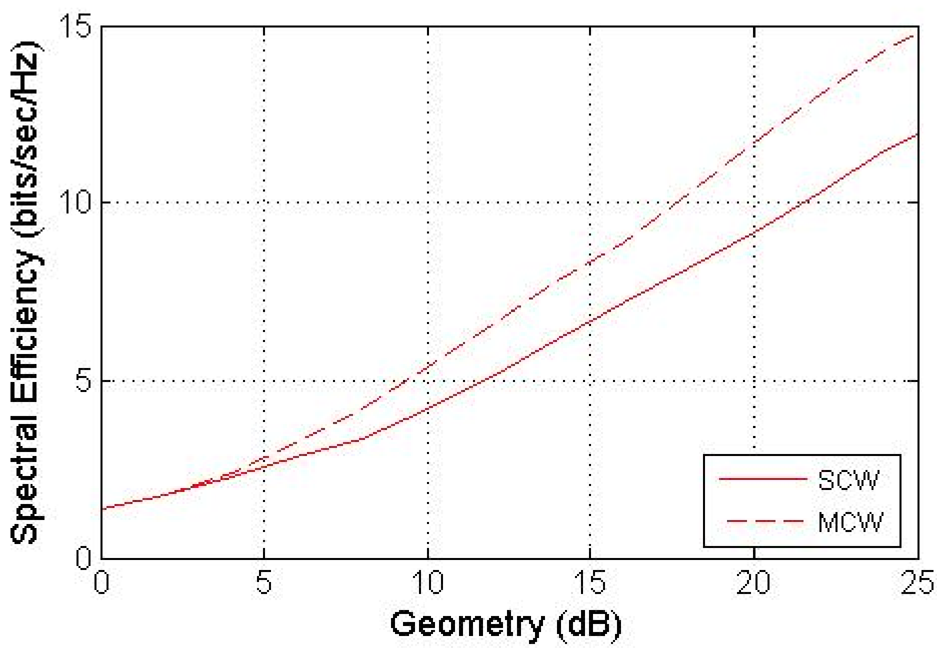

Figure 3-1 Spectral efficiency vs. SINR for 4x4 MCW and SCW MIMO with SCM suburban macro cell correlation model. Base station AoD 50 degree, AS 2 degree, PedB 3km/H.

3.2 Pseudo-eigenbeamforming for TDD MIMO

For TDD systems, the AP may have partial knowledgement of the forward link channel from reverse link pilots. Assuming the reverse link pilots can be transmitted through only one transmit antenna, the Pseudo-eigenbeamforming (Pseudo-EBF) technique [7] can be employed to enhance the MIMO performance. Figure 3-2 illustrates the potential gain of Pseudo-EBF in a 4x2 (i.i.d.) TDD MIMO system for PedB channel. The constrained capacity of SCW combined with Pseudo_EBF, SCW, 4x2 TDD beamforming, and 1x2 are shown in Figure 3-2. The capacity study assumes 3 dB gap to capacity to take into account coding and channel estimation loss. It is observed that Pseudo-EBF captures the beamforming gain (> 3dB) at low geometry while provides MIMO (spatial multiplexing) gain (2-3dB) at high geometry.

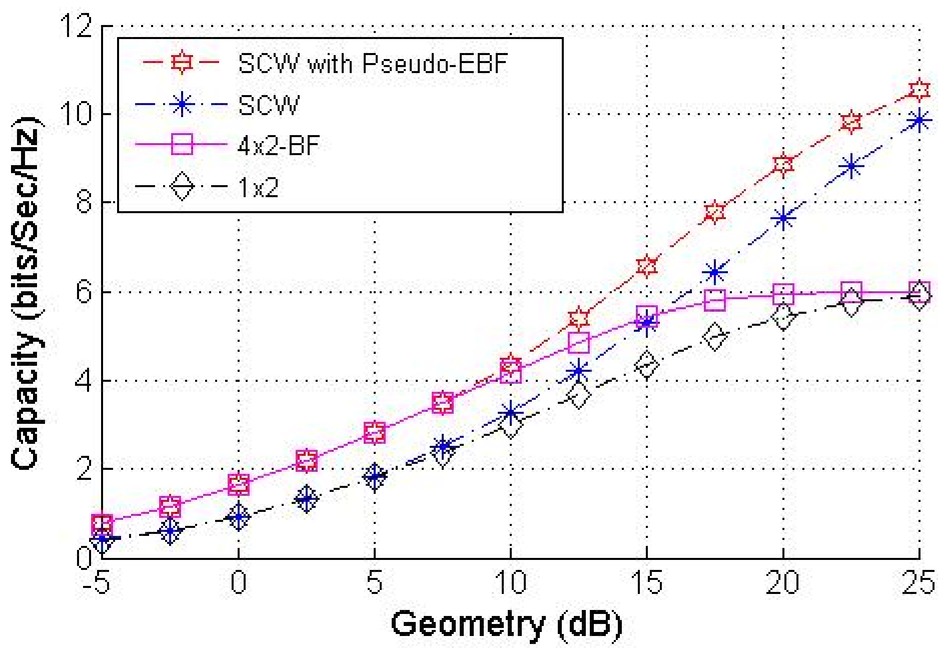

Figure 3-2 Constrained Capacity vs. SINR for i.i.d. 4x2 SCW MIMO with Pseudo-EBF

4 System Level Performance with Enhancement Features

In this section, we present performance results for the system level enhancement features. The enhancements include

- Quasi Orthogonal Reverse Link Operation
- Fractional Frequency Reuse Schemes
- Space Dimension Multiple Access (SDMA)
- Beamforming

4.1 Simulations Basic Assumptions

The system of 10MHz bandwidth deployments with Full Buffer traffic was simulated. The simulations used suburban macro cell channel models with pedB (3km/hr) and vehA (120 km/hr) multipath profiles as described in [3]. The baseline parameters for the FL/RL settings are listed in Table 4-1, and the numerology for baseline TDD operation is listed in Table 4-2.

Table 4-1 System Simulation Parameters (I)

	FL Evaluation	RL Evaluation
Network Topology	Hexagonal Grid, 19 cells with wrap around.	Hexagonal Grid, 19 cells with wrap around.
TDD Mode	1:1 (FL:RL)	1:1 (FL:RL)
Site-to-Site distance	1km, 2.5km	1km, 2.5km
Sectorization	3 sectors/cell	3 sectors/cell
Horizontal Antenna Pattern	70 deg@3dB bandwidth, 20dB maximum attenuation.	70 deg@3dB bandwidth, 20dB maximum attenuation.
Vertical Antenna Pattern	None	None
Propagation model.	Suburban macro 31.5+ $35\log_{10}$(d in m)dB Urban micro (NLOS) 34.53+ $38\log_{10}$(d in m)dB	Suburban macro 31.5+ $35\log_{10}$(d in m) dB Urban micro (NLOS) 34.53+ $38\log_{10}$(d in m)dB
BTS Minimum Separation	35m	35m
BTS Ant Height	32m(macro) / 12.5(micro)	32m(macro) / 12.5(micro)
AT Ant Height	1.5m	1.5m
Carrier Frequency	1.9GHz	1.9GHz
Bandwidth	10MHz	10MHz
Admission Control	None	None
Log-normal Shadowing	10dB	10dB
Site-to-site shadow correlation coefficient	0.5	0.5
Thermal Noise Density	-174dBm/Hz	-174dBm/Hz

		FL Evaluation	RL Evaluation
Noise Figure		10dB	5dB
Max Transmit Power		43dBm/MHz	27dBm
Peak base-station antenna gain with cable loss		17dBi-3dB = 14dBi	17dBi-3dB=14dBi
Penetration Loss		10dB(Veh)	10dB(Veh)
MS Antenna Gain		0dBi	0dBi
Body Losses		3dB	3dB
Maximum C/I achievable per antenna		30dB	30dB
BTS Antennas		1, 4 transmitter antennas	2, 4 receiver antennas
AT Antennas		2, 4 receiver antennas	1 transmitter antenna
ITU Channels		Suburban macro, pedB@3km/h, VehA,VehB@120km/h	Suburban macro, pedB@3km/h, VehA,VehB@120km/h
AT	Ant. Spacing	0.5λ	0.5λ
	Correlation	SCM suburban macro	SCM suburban macro
BTS	Ant. Spacing	0.5λ/10λ	10λ
	Correlation	SCM suburban macro	SCM suburban macro
Fairness		DV fairness (0.1, 0.1), (0.5, 0.5) normalized throughput line.	DV fairness (0.1, 0.1), (0.5, 0.5) normalized throughput line.
Traffic		Full Buffer	Full Buffer
Receiver Combining		MMSE	MMSE

Table 4-2 System Simulation Assumptions (II)

Parameters	TDD
Transmission Bandwidth	10MHz
Subcarrier Spacing	9.6kHz
Sampling Frequency	9.8304MHz
FFT Size	1024
Guard Carriers	32
Cyclic Prefix Length	6.51 μs
Windowing Duration	3.26 μs
OFDM Symbol Duration	113 μs
Number of OFDM Symbols Per Frame	8

4.2 Quasi Orthogonal Reverse Link

In this section, we present performance results for Quasi Orthogonal Reverse Link (QORL) operation as described in [7]. In QORL, by using a quasi-orthogonal multiplexing scheme where multiple ATs of the same sector are assigned the same bandwidth resources, the dimension limitation of capacity in orthogonal multiple access is mitigated. Spatial processing with multiple antennas at the AP is used to recover the overlapping signals from the different ATs. The proposed quasi-orthogonal scheme achieves intra-sector interference diversity through random hopping. With a standard orthogonal assignment scheme, the AP assigns to each AT within its sector a unique time-frequency block of subcarriers that are hopped in frequency across time. With QORL, the assignment to each AT may overlap with the assignments of one or more ATs on every time-frequency block. The sets of such interfering ATs will be different for subsequent blocks, hence providing a measure of co-channel interference diversity which is advantageously used by the H-ARQ scheme to terminate packet transmissions at an appropriate rate.

To allow for quasi orthogonal multiplexing, a channel tree that consists of Q identical sub-trees is used. The base nodes of each sub-tree are randomly mapped to the same set of time-frequency blocks, with the constraint that within each sub-tree, the base nodes map to disjoint resources. Within each block and at pre-defined time-frequency locations, Q sets of pilot symbols are orthogonally multiplexed to enable accurate estimation of the Q channels corresponding to the ATs multiplexed over that block.

We present numerical results for a multiplexing factor (Q) of 2 (and compare with the base line case of Q=1), however the proposed system supports a Q factor of up to 3. Note that these results are derived from our QFDD system study. However, since the control channel modeling in the QTDD system is similar to that in the QFDD system, and since for QORL channel reciprocity is not used, the gains in the QTDD system are expected to be similar to that in the QFDD system. Table 4-3 shows the sector throughput gains obtained by quasi orthogonal multiplexing with Q=2, in an urban micro deployment with site-to-site distance of 500m. Four diversity antennas with a spacing of 10λ are assumed to be used at the base station, with a single transmit antenna at each terminal. For spatial processing at the access point, only intra-sector interference nulling has been used. The additional channel estimation loss due to spatial processing at the access point has also been taken into account. As we can see, sector throughput gains of more than 25% gain in sector throughput can be achieved by using a quasi-orthogonal multiplexing of order 2 on the reverse link. Note that the QORL gains in these results are pessimistic due to the following suboptimal assumptions:

- Same multiplexing factor for all users including those in power limited regime.
- Users are randomly overlapping.

Table 4-3 Sector throughput gains obtained by quasi orthogonal multiplexing with Q=2 and 4Rx diversity antennas

Sector Throughput (Kbps)	QORL Gain
Pedestrian B at 3 Km/h	27%
Vehicular A at 30 Km/h	24%

4.3 Fractional Frequency Reuse

Simulation results demonstrating the capabilities of Fractional Frequency Reuse (FFR) [7] in the proposed system are shown in this section. The results show the system performance with 500 m site-to-site distance. Note that these results are derived from QFDD system simulation results. However, because there is no difference of applying FFR in the QTDD system or the QFDD system, the gains in the QTDD system are expected to be similar to that in the QFDD system. The geometry mentioned in Figure 4-1 corresponds to the long term C/I per antenna after frequency reuse is applied to edge users. The geometry is observed to improve as the partial loading factor increases.

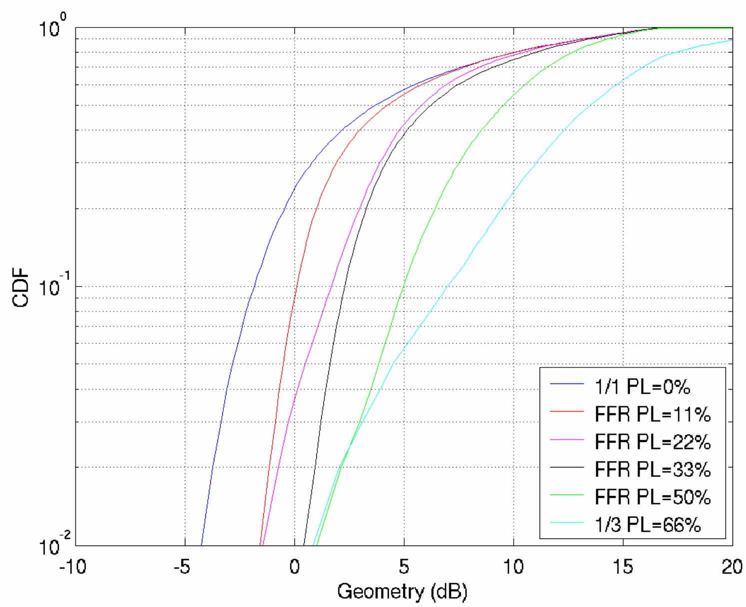

Figure 4-1 Geometry at 500m site-to-site distance for FFR with bandwidth partial loading from 0 to 66%

A dynamic FFR scheduler has been implemented to assign frequency reuse based on a packet-by-packet basis. The full buffer sector throughput and edge spectral efficiency tradeoffs through FFR are demonstrated in Table 4-4. It is observed that the edge spectral efficiency could improve 69% with a slight sector throughput loss of 8%. The edge user performance enhancement due to FFR is expected to have a significant impact on handoff and QoS.

Table 4-4 Proportional fairness full buffer simulations for 500 meter site-to-site with dual Rx diversity

	1/1 Reuse	FFR 11% PL	FFR 22% PL	FFR 33% PL	FFR 50% PL
Normalized Sector Throughput	1.00	1.02	0.98	0.92	0.76
Normalized 5% User Spectral efficiency	1.00	1.27	1.37	1.69	2.00

4.4 SDMA for QTDD System

In addition to the system level performance results presented in QTDD Performance Report 1 [6], we present the performance results of the QTDD system implementing SDMA feature. Multiplexing factor of 2 is considered in the simulations. No RL channel reciprocity is assumed and used for FL transmissions. Two spatially multiplexed beams centered at -30 degrees and 30 degrees relative to the antenna boresight are used for SDMA transmission. Based on their directions from the base station and their beamed geometry, each user will select a favorite beam to use. The base station will keep two users spatially multiplexed on their respective beams and simultaneously transmit to both using the same traffic channel. For each user, SIMO transmission is used. The ATs will then extract and decode their own intended packets using either MRC or MMSE receivers. Both receiver architectures are considered for the simulation, and they are explained below:

- MRC receiver: There is no estimation of the spatial structure of the interference.
- MMSE receiver: Perform spatial processing based on the estimate of spatial structure of the interference.

We present the simulation results of the system with SDMA for pedB channel at 3km/h in a suburban macro environment with cell sizes of 1km site-to-site distances. Four transmit antennas are used at the base station with 0.5λ spacing. Note that these results are derived from QFDD system simulation results. However, the SDMA gains in the QTDD system are expected to be similar to that in the QFDD system when no channel reciprocity is explored. The sector throughput gains of SDMA over the 1Tx baseline system are shown in Table 4-5, where the baseline system for 4x2 SDMA is a 1x2 SIMO system and the baseline system for 4x4 SDMA is a 1x4 SIMO system. It is observed that when MRC receiver is used, the QTDD SDMA system with multiplexing factor of 2 provides about 50% gain over the baseline single transmit antenna system. When spatial processing with MMSE receivers is used, the gains increase to about 75%~95% depending on the number of receiving antennas. Note that the SDMA gains in these results are pessimistic due to the following suboptimal assumptions:

- Two fixed beams are implemented in the simulations.
- Same SDMA multiplexing order for all users including those in power limited regime.
- Static SDMA assignment instead of packet-by-packet beam selection based on CQI feedback.
- No channel reciprocity is employed.

Since intra-sector interference depends on the beam of the overlapping user, if more beams are available and the scheduler uses appropriate beams to overlap users, additional SDMA gain will be expected.

Table 4-5 TDD FLSDMA Sector Throughput Gain

Sector Throughput Gain over 1Tx Baseline System	4x2		4x4	
	0.5λ Tx Spacing		0.5λ Tx Spacing	
	MRC	MMSE	MRC	MMSE
1km BS to BS Suburban Macro PedB 3km/h	47%	76%	49%	96%

4.5 Beamforming for QTDD System

QTDD system performance with the Beamforming feature enabled is evaluated in the simulations. The basic Beamforming assumptions are listed in Table 4-6. Cell sizes of 1 km and 2.5km site-to-site distance are considered. The system is loaded with 32 users per sector and simulated for suburban macro environment channel models with multipath profiles of pedB (3 km/hr) and vehA (120 km/hr).

Two types of scheduling fairness, namely, 802.20 fairness and Equal Grade of Service (EGoS) fairness, are considered in the simulations to examine the performance of Beamforming in high and low geometry settings. It is known that the Beamforming provides the most benefit when the user is primarily operating in a low geometry regions of the spectral efficiency curve. Capacity increases linearly with the power gains provided by Beamforming at low geometries while it only benefits logarithmically at high geometries. Therefore, it is useful to examine the effects of Beamforming to low geometry users when used in conjunction with EGoS scheduling.

Table 4-6 TDD Beamforming Simulation Parameters

Parameters		FL TDD Beamforming
RL Pilot Channel Modeling		Consistent with [5]
Channel Estimation Error with RL Pilot		-13dB
Calibration Error	Amplitude Variation (σ)	1dB
	Phase Variation (σ)	20 degree

4.5.1.1 802.20 Fairness Scheduling

In this section, we present system throughput results with an 802.20 fairness scheduler which meets the fairness criteria specified in the Evaluation Criteria [1]. The aggregated data rates for FL simulation with a 10 MHz block assignment are shown and compared to the baseline single antenna TDD system results in Table 4-7. The fairness plots with respect to mobile throughput in all simulations are shown in Figure 4-2 and Figure 4-3, and it is observed that they satisfy the fairness requirements in the Evaluation Criteria.

Scenarios of both correlated antennas with 0.5λ spacing and diversity transmit antennas with 10λ spacing at the base station are considered. In the case of correlated antennas with 0.5λ spacing at the base station, it is observed that Beamforming gain is about 60%~70% over the baseline single antenna system results for both pedB and vehA channels. For 10λ spacing, it is observed that for pedB channels at 3km/hr, Beamforming performance degradation compared to the performance of the 0.5λ spacing case is very small, on the order of 5%. However, for vehA channels at 120km/hr, due to the inaccuracy of tracking the FL channel based on RL pilots, most of the beamforming gain is lost in the diversity antennas of 10λ spacing case, and its performance is similar to that of the single antenna system.

Table 4-7 TDD FL Beamforming Sector Throughput

Sector Throughput (Kbps) and Gain over Baseline system		Beamforming			Baseline
		4x2		8x2	1x2
		0.5 λ (Tx)	10 λ (Tx)	0.5 λ (Tx)	
		MRC	MRC	MRC	MRC
1km BS to BS Suburban Macro	pedB 3km/h	9179 (59%)	8831 (53%)	9858 (71%)	5775
	vehA 120km/h	8484 (58%)	5268 (-2%)	8786 (64%)	5366
2.5km BS to BS Suburban Macro	pedB 3km/h	8948 (58%)	8348 (48%)	9717 (72%)	5659
	vehA 120km/h	8118 (61%)	4981 (-1%)	8375 (66%)	5048

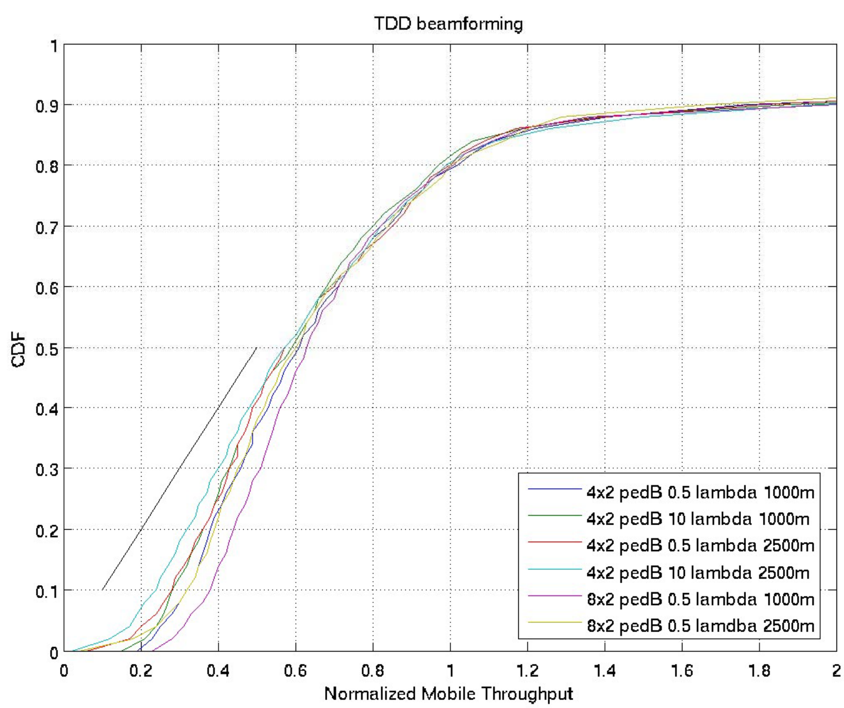

Figure 4-2 Fairness,TDD FL Beamforming, pedB 3km/hr, 32 users per sector

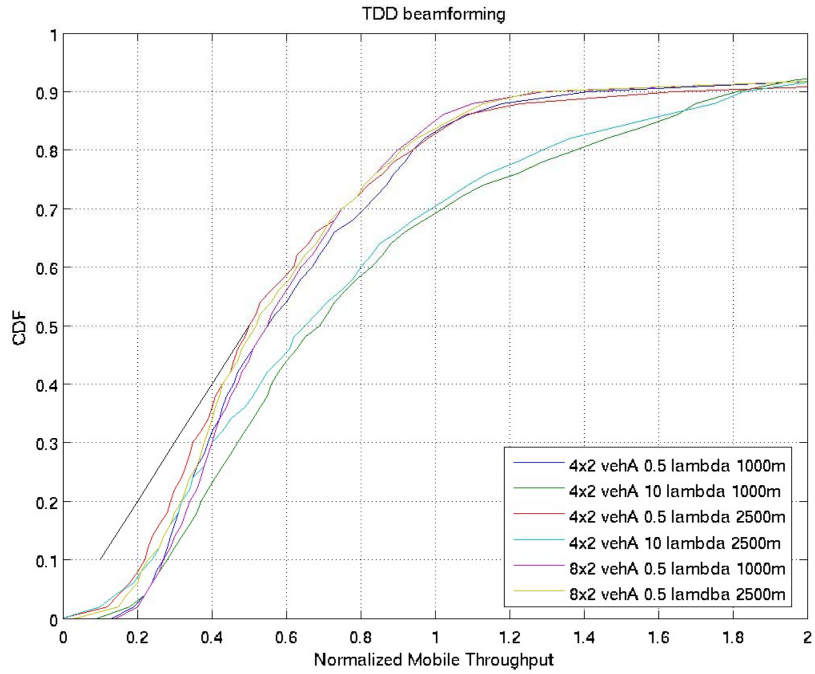

Figure 4-3 Fairness, TDD FL Beamforming, vehA 120km/hr, 32 users per sector

4.5.1.2 Equal Grade of Service Scheduling

We consider the forward link Beamforming performance with EGoS scheduling. The aggregated data rates for FL simulations with a 10 MHz block assignment are shown in Table 4-8. Fairness with respect to mobile throughput in all simulations are shown in Figure 4-4 and Figure 4-5. It is observed that Beamforming provides about 70~100% gain over the single antenna system results. As mentioned earlier, this gain is higher than the gains achieved with 802.20 fairness scheduling. This is because low geometry edge users benefit more from the beamforming gain, which significantly affects the overall system performance in the EGoS scheduling scenario. Similarly, the gain is higher in a large cell size than that in a smaller cell. For the vehA channel with high doppler, it is observed that, at 0.5λ transmit antenna spacing, most of the Beamforming gain is preserved; however, the gain is lost when the antenna spacings increase to 10λ.

Table 4-8 TDD FL Beamforming Sector Throughput

Sector Throughput (Kbps) and Gain over Baseline System		Beamforming			Baseline
		4x2		8x2	1x2
		0.5λ (Tx)	10λ (Tx)	0.5λ (Tx)	
		MRC	MRC	MRC	MRC
1km BS to BS Suburban Macro	pedB 3km/h	6816 (70%)	5986 (50%)	8219 (105%)	4000
	vehA 120km/h	5423 (82%)	3418 (15%)	5958 (100%)	2973
2.5km BS to BS Suburban Macro	pedB 3km/h	5928 (98%)	5338 (78%)	7214 (141%)	2993
	vehA 120km/h	4681 (95%)	2785 (16%)	5217 (117%)	2406

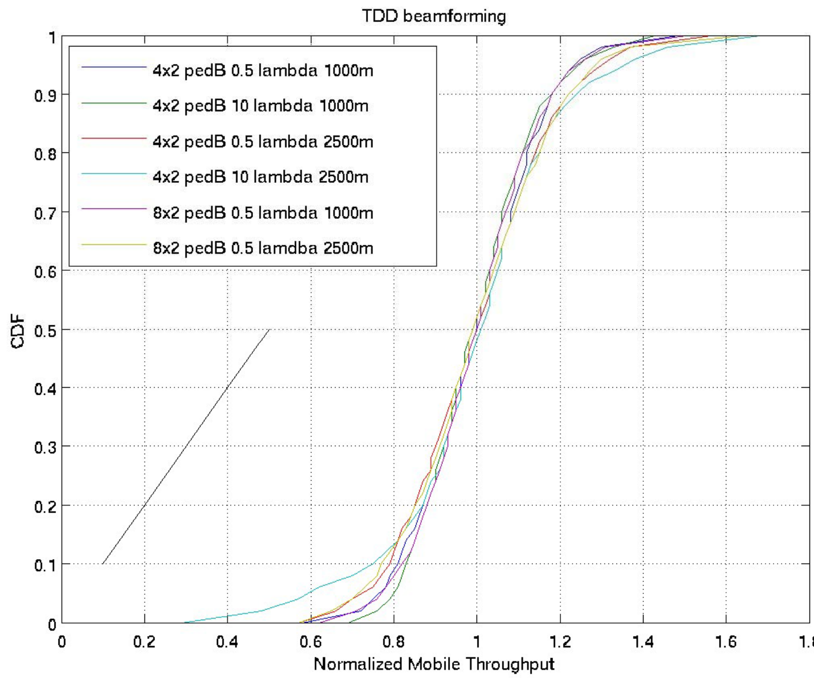

Figure 4-4 Fairness, TDD FL Beamforming, pedB 3km/h

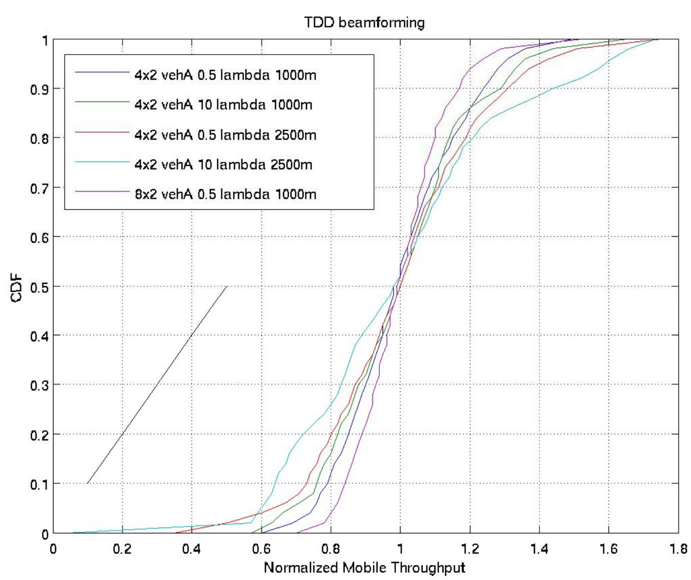

Figure 4-5 Fairness, TDD FL Beamforming, vehA 120km/h

5 References

[1] IEEE 802.20 – "The approved version of the Evaluation Criteria Document (ECD)," 802.20-PD-09.

[2] IEEE 802.20 – "The approved System Requirements Document (SRD)," 802.20-PD-06r1.

[3] IEEE 802.20 – "The adopted Channel Models Document," 802.20-PD-08.

[4] IEEE 802.20 – "Technology Selection Procedure," 802.20-PD-08.

[5] IEEE 802.20 – "QFDD and QTDD: Proposed Draft Air Interface Specification," C802.20-05/69.

[6] IEEE 802.20 – "QTDD Performance Report 1," C802.20-05/61r1.

[7] IEEE 802.20 – "QFDD and QTDD: Technology Overview," IEEE C802.20-05/68.

[8] IEEE_C802.20-05/65 – QTDD Requirements Compliance Report, Jim Tomcik, October 28, 2005.

[9] ITU Recommendation G.107 – The E-model, a computational model for use in transmission planning.

[10] ITU Recommendation G.729A – Appendix A: Reduced complexity 8 kb/s CS-ACELP Codec for Digital Simultaneous Voice and Data.